NOTICE

CERTAIN DATA CONTAINED IN THIS DOCUMENT MAY BE DIFFICULT TO READ IN MICROFICHE PRODUCTS.

LA-UR 91-2965

LA-UR--91-2965

DE92 000220

Los Alamos National Laboratory is operated by the University of California for the United States Department of Energy under contract W-7405-ENG-36.

TITLE: ALGEBRAIC CALCULATION OF STROBOSCOPIC MAPS OF ORDINARY, NONLINEAR DIFFERENTIAL EQUATIONS

AUTHOR(S): R. WACKERBAUER, A. HUBLER and G. MAYER-KRESS

SUBMITTED TO: The Proceedings of the CNLS 11th Annual Conference "Experimental Mathematics: Computational Issues in Nonlinear Science" held in Los Alamos May 20-24, 1991

DISCLAIMER

Los Alamos Los Alamos National Laboratory
Los Alamos, New Mexico 87545

FORM NO 836 R4
ST NO 2629 5/81

CNLS 91-W01

Algebraic Calculation of Stroboscopic Maps of Ordinary, Nonlinear Differential Equations

R. Wackerbauer

Max-Planck-Institut für extraterrestrische Physik, W-8046 Garching, Germany

A. Hübler

Center for Complex Systems Research, University of Illinois, Urbana, IL 61801, USA

G. Mayer-Kress

Center for Nonlinear Studies, Los Alamos National Laboratory, Los Alamos NM 87545

and Department of Mathematics, University of California at Santa Cruz

July 25, 1991

Abstract

The relation between the parameters of a differential equation and corresponding discrete maps are becoming increasingly important in the study of nonlinear dynamical systems. Maps are well adopted for numerical computation and several universal properties of them are known. Therefore some perturbation methods have been proposed to deduce them for physical systems, which can be modeled by an ordinary differential equation (ODE) with a small nonlinearity. A new iterative, rigorous algebraic method for the calculation of the coefficients of a Taylor expansion of a stroboscopic map from ODE's with not necessarily small nonlinearities is presented. It is shown analytically that most of the coefficients are small for a small integration time and grow slowly in the course of time if the flow vector field of the ODE is polynomial and if the ODE has fixed point in the origin. Approximations of different orders respectively of the rest term are investigated for several nonlinear systems.

1 Introduction

The motion of the driven Helmholtz oscillator [1], of a van der Pol oscillator [2], and many other nonlinear dynamical systems show complex long time behavior, but smooth short time dynamics. In this case the topological structure of the trajectories of the continuous and the discrete system is equivalent [3]. Also the motion of the planets can be described in a good approximation by a fast rotation around the sun on elliptic orbits, where the eccentricity and the point of culmination change comparatively slowly but with a complex long time dynamics. Is the motion of the point of culmination chaotic, periodically oscillating, stable or unstable, the whole dynamics possesses this property. Poincaré and others [4,5,6] have shown that the parameter dependence of those dynamical systems can be described easier by means of iteration functions, which describes e.g. the dynamics of the point of culmination of a trajectory, than by the original differential equation. Especially if the amplitude frequency coupling (AF-coupling) [7] of a nonlinear oscillator is complicated, a Poincaré map may be comparatively simple, since it is insensitive to the AF-coupling, if the Poincaré surface is properly chosen. Recently, stroboscopic maps have become important, since it has been shown that they are insensitive on the AF-coupling too after an appropriate rescaling of the flow vector field of the corresponding ODE, and since they can be calculated by some algebraic methods. [5,6,9] All these methods start from the assumption that the strength of the nonlinearity is expressed by a parameter ϵ. In perturbation theory the exact solution is expanded with respect to ϵ for small ϵ. The resulting solutions are valid for a large class of initial states but only for small ϵ. Recently it has been shown [5,8,9,10] that even for large ϵ stroboscopic maps may be approximated with high accuracy by a polynomial of low degree for initial states in the neighborhood of an attractor. Feigenbaum [12] and others [13,14,16] have demonstrated that the parameter dependence of those maps may have universal properties if the higher order contributions are small enough. Therefore it seems useful to expand the exact solution of the ODE with respect to the initial states in the neighborhood of an attractor and calculate the leading coefficients of the expansion algebraically. If the resulting contributions of higher orders are small, a stroboscopic map which just takes into account the leading coefficients should qualitatively reproduce the parameter dependence of the dynamics of the ODE. Additionally a method for just the opposite way, to construct a class of suspensions and autonomous differential equations for diffeomorphisms in the plane is already known [15]. In this paper we present a rigorous algebraic method to calculate the relation between coefficients of a Taylor expansion of a stroboscopic map and the parameters of the ODE

in closed form. In Sec.2 we present the algorithm and argue that the Taylor expansion of the stroboscopic map converges quickly for short intervals of integration time if the flow vector field of the ODE is a polynomial and has a fixed point in the origin. These conditions are fulfilled e.g. by the oscillators of Lorenz [17], Rössler [18], van der Pol [2] etc.. In sec. 3 we compare the bifurcation sets of forced Helmholtz's oscillator respectively the limit cycle behavior of van der Pol's oscillator resulting from a numerical integration and from the algebraic algorithm using a first order approximation. Furthermore in sec. 4.5 we demonstrate some results in the case of van der Pol's and Rössler's system using approximations of higher orders or approximations of the rest term, caused by truncation of the Taylor series. In sec.6 we discuss the connection between mathematical properties of the algebraic method and physical properties of dynamical systems. Finally in sec.7 we present some concluding remarks and suggestions for future directions.

2 Algebraic Calculation of Stroboscopic Maps

Consider a system of ordinary differential equations in $\mathbf{R}^n$

$$\dot{\underline{x}} = \underline{f}(\underline{x}(t)) \tag{1}$$

where $\underline{x}(t) \in \mathbf{R}^n$ is called state vector and $\underline{f} : \mathbf{R}^n \to \mathbf{R}^n, \underline{x} \mapsto \underline{f}(\underline{x})$ is the corresponding n dimensional flow vector field, assumed to be a polynomial. Therefore the j-th component of the flow vector field $\underline{f}$ can be represented as:

$$f_j = \sum_{\underline{l}=\underline{0}}^{\underline{d}_j} c_{j,\underline{l}} \prod_{i=1}^{n} x_i^{l_i} \qquad j = 1, \ldots, n \tag{2}$$

where $\underline{l} \in \mathbf{N}_0^n$ is an index vector and the components of the vector $\underline{d}_j \in \mathbf{N}_0^n$ fulfill the condition: $\sum_{i=1}^{n} d_{j_i} = g_j \equiv$ degree of the polynomial f_j.
Assuming $\underline{f}(\underline{0}) = \underline{0}$. This is no restriction as we can demonstrate for many cases [21]. There exists a transformation in an equivalent system of this form (for example Helmholtz's oscillator(chapt.3) or the Rössler system (chapt.5)).
Definition 2.1: Let $\underline{x}(t)$ represent a solution to the ODE under investigation. Then for fixed $T \in \mathbf{R}$ a mapping

$$\underline{S}_T : \mathbf{R}^n \to \mathbf{R}^n, \underline{x}(t) \mapsto \underline{x}(t+T) \tag{3}$$

is called *stroboscopic map* of strobe time T.

Using Eq.(1) and (3) we obtain a differential equation for the dynamics of the stroboscopic map.

$$\frac{d}{dT}\underline{x}(T) = \frac{d}{dT}\underline{S}_T(\underline{x}_0) := \dot{\underline{S}}_T(\underline{x}_0) = \underline{f}(\underline{S}_T(\underline{x}_0)) \tag{4}$$

where

$$\underline{S}_0(\underline{x}_0) = \underline{x}_0 := \underline{x}(0) \tag{5}$$

is the initial condition of the system. Thus we can formulate the identity: $\underline{S}_0(\cdot) = \underline{id}$
Recently it has been demonstrated that the stroboscopic map of some non-linear systems can be approximated with high accuracy by a polynomial of

low order in the initial values of the system [8,5]. Therefore we take a Taylor expansion as an ansatz for each component j of the stroboscopic map:

$$S_{j,T}(\underline{x}_0) = \sum_{\underline{m}=\underline{0}}^{\infty} a_{j,\underline{m}}(T) \prod_{\alpha=1}^{n} x_{0_\alpha}^{m_\alpha} \qquad \underline{m} \in \mathbf{N}_0^n \qquad j = 1, \ldots, n \tag{6}$$

where $x_{0_\alpha} \in \mathbf{R}$ are the components of the initial state vector $\underline{x}_0$. The dynamics of the system is now represented by the time dependence of the mode amplitudes $a_{j,\underline{m}}(T) \in \mathbf{R}$.

Definition 2.2: The *order of a mode* $a_{j,\underline{m}} \in \mathbf{R}$ is given by $\|\underline{m}\|_1 = \sum_{i=1}^{n} m_i$.

Remark 2.1: Constant, linear respectively nonlinear modes are of order $\|\underline{m}\|_1 = 0, 1$, respectively > 1.

Lemma 2.1: Let $f_j(\underline{x}) \in \mathbf{R}$ be analytical functions in the state variables $x_i \in \mathbf{R}$ for $i, j = 1, 2, \ldots, n$
then $S_{j,T}(\underline{x}_0) = x_j$ are analytical functions of their arguments, in some neighborhood of each value and therefore there exists a $T > 0$ such, that $S_{j,T}(\underline{x}_0)$ converges
For a *proof* see [19] and [20].

Theorem 2.1: Let $\underline{f}, \underline{S}_T \in \mathbf{R}^n$ be polynomials as defined in Eq.(2,6), let $(i, \beta) \in \mathbf{N} \times \mathbf{N}_0$ be an index of the index vector $\underline{k} \in \mathbf{N}_0^n$, let $\underline{m} \in \mathbf{N}_0^n$, then the dynamics of $a_{j,\underline{m}}(T) \in \mathbf{R}, j = 1, 2, \ldots, n$ is given by

$$\dot{a}_{j,\underline{m}}(T) = \sum_{l=\underline{0}}^{\underline{d}_j} c_{j,l} \sum_{\substack{\underline{k}^{(i,\beta)} = \underline{0} \\ 0 \le \beta \le l_i \\ 1 \le i \le n}}^{\infty} \left[\prod_{i=1}^{n} \prod_{\beta=0}^{l_i} a_{i,\underline{k}^{(i,\beta)}}(T) \delta_{\underline{m}, \sum_{i=1}^{n} \sum_{\beta=0}^{l_i} \underline{k}^{(i,\beta)}} \right] \tag{7}$$

proof: Using Eq.(3), Eq.(7) can be derived from Eq.(4) by equating the coefficients of like powers in the initial values. See [21] for details.

Remark 2.2: Because $l_i = 0$ is possible, the running index $\beta \in \mathbf{N}_0$ starts with $\beta = 1 - \delta_{0,l_i}$. This involves the requirement for $\beta = 0$:$\underline{k}^{(i,0)} := \underline{0}$ and $a_{i,\underline{k}^{(i,0)}} := 1$ to get the right general formula for the mode amplitudes. Therefore in consideration of this requirement $\beta \in \mathbf{N}_0$ can always start with $\beta = 0$. In the following we argue that Eq.(6) is determined by only a few coefficients for small T. Afterwards we will solve Eq.(7) in a closed form.

Lemma 2.2: Let $\underline{S}_0(\cdot) \in \mathbf{R}^n$ be the identity operator, then the radius of convergence of the stroboscopic map $\underline{S}_T \in \mathbf{R}^n$ is infinite for $T = 0$.

proof: Due to Eq.(5) we obtain

$$a_{j,\underline{m}}(0) = \delta_{1,m_j} \prod_{\alpha \neq j} \delta_{0,m_\alpha} \qquad \forall \quad \alpha, j = 1, \ldots, n \tag{8}$$

Remark 2.3: For a n-dimensional system only n linear modes $a_{j,\underline{m}} \in \mathbf{R}$ do not vanish for $T = 0$.

Lemma 2.3: For $T = 0$ the radius of convergence of the time derivative of the stroboscopic map $\dot{\underline{S}}_0(\underline{x}_0) \in \mathbf{R}^n$ map is infinite for $T = 0$.

proof: Eq.(7) leads to

$$\dot{a}_{j,\underline{m}}(0) = \sum_{\underline{l}=\underline{0}}^{\underline{d}_j} c_{j,\underline{l}} \prod_{\alpha=1}^{n} \delta_{m_\alpha,l_\alpha} \qquad \forall \quad j = 1,\ldots,n \tag{9}$$

Thus, caused by the Kronecker-delta in Eq.(9), $\dot{a}_{j,\underline{m}}(0) \neq 0$ for all $\underline{m}$ which correspond to such index vector $\underline{m} = \underline{l}$ with $c_{j,\underline{l}} \neq 0$.

Due to Eq.(8) nearly all modes vanish at time $T = 0$ and due to Eq.(9) only a few modes change their amplitude at time $T = 0$. So Eq.(9) indicates that all other modes remain small for small strobe times T. Therefore we have the following definition:

Definition 2.3: Let $a_{j,\underline{\mu}} \in \mathbf{R}$ be characterized by a non changing amplitude at $T = 0$: $\dot{a}_{j,\underline{\mu}}(0) \neq 0$ for some $j = 1,2,\ldots,n$, then $a_{j,\underline{\mu}} \in \mathbf{R}$ is called *important mode* $\forall \quad j = 1,2,\ldots,n$.

Definition 2.4: The stroboscopic map $\underline{S}_T \in \mathbf{R}^n$, consisting of all linear modes and only the important nonlinear modes is called *first order approximation of* $\underline{S}_T$: $\underline{S}_T^{(1)}(\underline{x}_0)$

For $n > 1$ a *n-th order approximation*: $\underline{S}_T^{(n)}(\underline{x}_0)$ consists of all modes of order $\|\underline{m}\|_1 = n$.

Lemma 2.4: Let $a_{j,\underline{\mu}} \in \mathbf{R}$ be an important mode and $g_j = \sum_{i=1}^{n} d_{j_i} \in \mathbf{R}$ the degree of the flow vector field $f_j \in \mathbf{R}$, then the maximum order of $a_{j,\underline{\mu}}$ and $i, j = 1,2,\ldots,n$ is given by: $\|\underline{\mu}\|_{1,max} = max\{g_j | j = 1,\ldots,n\}$

proof: Due to Eq.(9) each nonlinear term with coefficient $c_{j,\underline{l}} \in \mathbf{R}$ of the flow vector field $\underline{f}$ corresponds definitely to one important mode $a_{j,\underline{l}}(T)$.

Finally we argue that the relation between the coefficients of the flow vector field $c_{j,\underline{l}} \in \mathbf{R}$ and the coefficients of the Taylor expansion of a stroboscopic map $a_{j,\underline{m}} \in \mathbf{R}$ can be calculated in closed form.

Definition 2.5: The structure of modes $a_{j,\underline{m}} \in \mathbf{R}$ is called *hierarchically*, if a mode $a_{j,\underline{m}}$ only depends on modes $a_{\alpha,\underline{k}^{(i,\beta)}}$, where all components of the index vector $\underline{k}^{(i,\beta)} \in \mathbf{N}_0^n$ are less or at most equal than the corresponding components of the vector $\underline{m} \in \mathbf{N}_0^n$. Or in other words, if modes of higher order can iteratively be calculated from the lower ones with a recursion formula.

Lemma 2.5 evt. Theorem 2.2: Eq.(7) is a hierarchical system of differential equations.

proof: With $k_\alpha^{(i,\beta)} \in \mathbf{N}_0$ the $\delta-$function in Eq.(7) leads to $k_\alpha^{(i,\beta)} \leq m_\alpha$ $\forall \quad \alpha = 1,2,\ldots,n$

Lemma 2.6 evt. Theorem 2.3: Consider Eq.(1,2) and let $c_{j,\underline{0}} = 0 \quad \forall \quad j =$

$1, 2, \ldots, n$ which is equivalent to the fixed point behavior $\underline{f}(\underline{0}) = \underline{0}$ then Eq.(7) becomes a linear differential equation with constant coefficients $c_{j,\underline{l}} \in \mathbf{R}$.

proof: Due to Eq.(7.8) the assumption $c_{j,\underline{0}} = 0$ leads to $a_{j,\underline{0}}(T) \equiv 0$ $\forall \quad j = 1, 2, \ldots, n$ By this Eq.(7) is a linear differential equation with constant coefficients and an inhomogeneity consisting of products of modes of only lower order than $\|\underline{m}\|_1$, which are known caused by the hierarchic principle of the mode equations. For a more detailed proof, see [21].

In this chapter the differential equations of modes are reduced to a linear, inhomogeneous, n-dimensional system of differential equations with constant coefficients, which is analytically solvable [22]. In the next sections this method will be applied to calculate the bifurcation set of Helmholtz's oscillator or the phase space dynamics of van der Pol's and Rössler's system.

3 First Order Approximations of the Stroboscopic Map

3.1 The stroboscopic map of Helmholtz's oscillator

Consider forced oscillations in the potential $V_\gamma(x)$ of the form

$$\ddot{x} + \epsilon\dot{x} + \frac{d}{dx}V_\gamma(x) = f\cos(\omega t) \tag{10}$$

where $\epsilon > 0$ is the damping constant, $\gamma \in \mathbf{R}$ quantifies the form of the potential and f, ω frequency and amplitude of external forcing.
The special potential of Helmholtz's system

$$V_\gamma(x) = \frac{\gamma}{2}x^2 + \frac{1}{3}x^3 \tag{11}$$

shows oscillatory behavior in the case of $\epsilon^2 - 4\gamma < 0$ (complex eigenvalues).
Eq. (10) can be transformed in a system of first order differential equations

$$\begin{pmatrix} \dot{x}_1 \\ \dot{x}_2 \\ \dot{x}_3 \\ \dot{x}_4 \end{pmatrix} = \begin{pmatrix} 0 & 1 & 0 & 0 \\ -\gamma & -\epsilon & 1 & 0 \\ 0 & 0 & 0 & 1 \\ 0 & 0 & -\omega^2 & 0 \end{pmatrix} \begin{pmatrix} x_1 \\ x_2 \\ x_3 \\ x_4 \end{pmatrix} - \begin{pmatrix} 0 \\ x_1^2 \\ 0 \\ 0 \end{pmatrix} \tag{12}$$

In this representation the flow vector field $\underline{f} \in \mathbf{R}^4$ of Eq. (12) is a polynomial with a fixed point in the origin, as provided in the last chapter.
With the ansatz

$$S_{j,T}(\underline{x}_0) = \sum_{\substack{m_1,m_2 \\ m_3,m_4=0}}^{\infty} a_{j,\underline{m}}(T) x_{0_1}^{m_1} x_{0_2}^{m_2} x_{0_3}^{m_3} x_{0_4}^{m_4} \tag{13}$$

we obtain a linear hierarchic system of differential equations with constant coefficients describing the dynamics of the mode amplitudes.

$$\begin{pmatrix} \dot{a}_{1,\underline{m}} \\ \dot{a}_{2,\underline{m}} \\ \dot{a}_{3,\underline{m}} \\ \dot{a}_{4,\underline{m}} \end{pmatrix} = \begin{pmatrix} 0 & 1 & 0 & 0 \\ -\gamma & -\epsilon & 1 & 0 \\ 0 & 0 & 0 & 1 \\ 0 & 0 & -\omega^2 & 0 \end{pmatrix} \begin{pmatrix} a_{1,\underline{m}} \\ a_{2,\underline{m}} \\ a_{3,\underline{m}} \\ a_{4,\underline{m}} \end{pmatrix} - \begin{pmatrix} 0 \\ \sum_{\underline{l},\underline{k}=\underline{0}}^{\infty} a_{1,\underline{l}} a_{1,\underline{k}} \delta_{\underline{m},\underline{l}+\underline{k}} \\ 0 \\ 0 \end{pmatrix} \tag{14}$$

$\underline{m}, \underline{l}, \underline{k} \in \mathbf{N}_0^4$

Applying the identity of $\underline{S}_T \in \mathbf{R}^n$ respectively the corresponding condition for the modes (Eq.(8))

$$a_{j,\underline{m}}(0) = \delta_{1,m_j} \prod_{\alpha \neq j} \delta_{0,m_\alpha} \tag{15}$$

the coefficients $a_{j,\underline{m}} \in \mathbf{R}^4$ of the stroboscopic map $\underline{S}_T \in \mathbf{R}^4$ are determined. Fig.(1) demonstrates that for small T only few modes do not vanish and only the amplitude of the important nonlinear mode is not small, which corresponds to Lemma 2.2 and Eq.(9) in chapt.2. Thus a first order approximation of the stroboscopic map $\underline{S}_T$ for the Helmholtz system is successive for about $T \leq \frac{\pi}{2}$.

Therefore the algebraic expression for this first order approximation including only the linear and important nonlinear modes $\underline{m} = (2,0,0,0)$ is derived, provided that $\omega = 1$.

$$\begin{aligned}
\mathbf{S}^{(1)}_{1,\mathbf{T}}(\mathbf{X_0}) &= \frac{D_2 e^{D_1 T} - D_1 e^{D_2 T}}{D_2 - D_1}\mathbf{X_{0_1}} + \frac{e^{D_2 T} - e^{D_1 T}}{D_2 - D_1}\mathbf{X_{0_2}} \\
&+ \left(\frac{[\epsilon - D_2(\gamma-1)]e^{D_1 T} + [-\epsilon + D_1(\gamma-1)]e^{D_2 T}}{(D_2 - D_1)N} + \frac{e^{iT}}{2(i\epsilon + \gamma - 1)} + \frac{e^{-iT}}{2(\gamma - 1 - i\epsilon)}\right)\mathbf{X_{0_3}} \\
&+ \left(\frac{(D_2\epsilon - \gamma + 1)e^{D_1 T} - (D_1\epsilon + \gamma - 1)e^{D_2 T}}{(D_2 - D_1)N} - \frac{ie^{iT}}{2(i\epsilon + \gamma - 1)} + \frac{ie^{-iT}}{2(\gamma - 1 - i\epsilon)}\right)\mathbf{X_{0_4}} \\
&+ \frac{1}{(D_2 - D_1)^2}\left(\frac{3D_1^2 - 2D_2^2 - D_1 D_2}{D_1(2D_2 - D_1)}e^{D_1 T} + \frac{3D_2^2 - 2D_1^2 - D_1 D_2}{D_2(2D_1 - D_2)}e^{D_2 T}\right. \\
&+ \left. 2e^{(D_1+D_2)T} - \frac{D_2^2}{D_1(2D_1 - D_2)}e^{2D_1 T} - \frac{D_1^2}{D_2(2D_2 - D_1)}e^{2D_2 T}\right)\mathbf{X^2_{0_1}} \\
\mathbf{S}^{(1)}_{2,\mathbf{T}}(\mathbf{X_0}) &= \frac{D_2 D_1}{D_2 - D_1}(e^{D_1 T} - e^{D_2 T})\mathbf{X_{0_1}} + \frac{D_2 e^{D_2 T} - D_1 e^{D_1 T}}{D_2 - D_1}\mathbf{X_{0_2}} \\
&+ \left(\frac{[\epsilon - D_2(\gamma-1)]D_1 e^{D_1 T} + [-\epsilon + D_1(\gamma-1)]D_2 e^{D_2 T}}{(D_2 - D_1)N} + \frac{ie^{iT}}{2(i\epsilon + \gamma - 1)} - \frac{ie^{-iT}}{2(\gamma - 1 - i\epsilon)}\right)\mathbf{X_{0_3}} \\
&+ \left(\frac{(D_2\epsilon + \gamma - 1)D_1 e^{D_1 T} - (D_1\epsilon + \gamma - 1)D_2 e^{D_2 T}}{(D_2 - D_1)N} + \frac{e^{iT}}{2(i\epsilon + \gamma - 1)} + \frac{e^{-iT}}{2(\gamma - 1 - i\epsilon)}\right)\mathbf{X_{0_4}} \\
&+ \frac{1}{(D_2 - D_1)^2}\left(\underbrace{\frac{3D_1^2 - 2D_2^2 - D_1 D_2}{D_1(2D_2 - D_1)}D_1}\, e^{D_1 T} + \underbrace{\frac{3D_2^2 - 2D_1^2 - D_1 D_2}{D_2(2D_1 - D_2)}D_2}\, e^{D_2 T}\right. \\
&+ \left. 2(D_1 + D_2)e^{(D_1+D_2)T} - \frac{2D_2^2}{2D_1 - D_2}e^{2D_1 T} - \frac{2D_1^2}{2D_2 - D_1}e^{2D_2 T}\right)\mathbf{X^2_{0_1}} \\
\mathbf{S}^{(1)}_{3,\mathbf{T}}(\mathbf{X_0}) &= \cos T\ \mathbf{X_{0_3}} + \sin T\ \mathbf{X_{0_4}} \\
\mathbf{S}^{(1)}_{4,\mathbf{T}}(\mathbf{X_0}) &= -\sin T\ \mathbf{X_{0_3}} + \cos T\ \mathbf{X_{0_4}}
\end{aligned}$$

$N = (\gamma - 1)^2 + \epsilon^2$ and $D_{1/2} = -\epsilon/2 \pm i\sqrt{4\gamma - \epsilon^2}/2$ are two eigenvalues of the linearized system.

The complicated dependence of the oscillation parameter ϵ, γ becomes evident in this map. Note, this is already true for the driven harmonic oscillator, as seen in the linearized map above.

In Fig.(2) we show a numerical comparison of the bifurcation sets of this algebraic map $S^{(1)}_{\frac{\pi}{2}}(\underline{x}_0)$ and the bifurcation set of Eq.(10), calculated with a Runge-Kutta method [25]. Note that only the nonlinear modes with index vector $\underline{m} = (2,0,0,0)$ have been included for this good qualitative agreement.

Figure 1: Time dependence of the mode amplitudes $a_{2,\underline{m}}(T)$ of Helmholtz's oscillator ($\gamma = 0.5, \epsilon = 0.3, \|\underline{m}\|_1 \leq 2$) whereby the coefficients of the first order approximation are specially signed: (linear ones: [1] : $a_{2,(1,0,0,0)}$, [2] : $a_{2,(0,1,0,0)}$, [3] : $a_{2,(0,0,1,0)}$, [4] : $a_{2,(0,0,0,1)}$ and the important one: [5] : $a_{2,(2,0,0,0)}$

Figure 2: Bifurcation diagrams of Helmholtz's oscillator ($\gamma = 0.5, \omega = 1$): First component of $S_{2\pi n}(\underline{x}_0)$ as a function of the force parameter f for various damping coefficients ϵ. ($n \in \mathbf{N}, x_{0_1} = -0.5, x_{0_2} = 0.1, x_{0_3} = f, x_{0_4} = 0$) a) Runge-Kutta-method b) algebraic, first order approximation: $S^{(1)}_{1,\frac{\pi}{2}}(\underline{x}_0)$

3.2 Stroboscopic Map of van der Pol's Oscillator

The differential equation of van der Pol's oscillator describes a nonlinear system with an amplitude-depending damping coefficient.

$$\ddot{x} - \epsilon(1 - x^2)\dot{x} + x = 0 \qquad 0 \leq \epsilon < 2 \tag{16}$$

Eq.(16) can be written as a first order system, where $\underline{f}(\underline{0}) = \underline{0}$ is automatically fulfilled.

$$\begin{pmatrix} \dot{x}_1 \\ \dot{x}_2 \end{pmatrix} = \begin{pmatrix} 0 & 1 \\ -1 & \epsilon \end{pmatrix} \begin{pmatrix} x_1 \\ x_2 \end{pmatrix} - \epsilon \begin{pmatrix} 0 \\ x_1^2 x_2 \end{pmatrix} \tag{17}$$

Again the corresponding equations describing the motion of the amplitudes $a_{j,nm} \in \mathbf{R}^2$ are hierarchic, linear with constant coefficients and inhomogeneous.

$$\begin{pmatrix} \dot{a}_{1,nm} \\ \dot{a}_{2,nm} \end{pmatrix} = \begin{pmatrix} 0 & 1 \\ -1 & \epsilon \end{pmatrix} \begin{pmatrix} a_{1,nm} \\ a_{2,nm} \end{pmatrix} - \epsilon \begin{pmatrix} 0 \\ \sum_{i,j,k,l=0}^{\infty} a_{1,kl} a_{1,ij} a_{2,\ldots} \end{pmatrix}$$

As a result we will compare numerically calculated limit cycles [24] with the corresponding algebraic calculated phase plots; for the algebraic calculation a map of first order is iterated; where first order means in the case of van der Pol's oscillator a map consisting of all linear modes and the important nonlinear modes $\underline{m} = (2, 1)$. For several strobe times $T > 0$ the periodic motion is demonstrated in Fig. (3,4). Even for larger damping constants the qualitative limit cycle behavior can be reproduced with this low order approximation, for example $\epsilon = 1.7$ in Fig. (4).
For special strobe times T we get good agreement of approximated limit cycles and numerical ones. Further, as will be shown below for the van der Pol system and Rössler's system these quantitative discrepances disappear if higher order contributions are used or if all higher order modes are estimated by a linear rest term.

Figure 3: Limit cycles of van der Pol's oscillator ($x_{0_1} = 0.. x_{0_2} = 2$) for $a)\epsilon = 0.3, b)\epsilon = 0.5$, numerically calculated [0], algebraic: first order approximation $\underline{S}_T^{(1)}(\underline{x}_0)$ for different T, using the symbols: [1] : $T = 0.1$, [2] : $T = 0.3$, [3] : $T = 0.5$, [4] : $T = 0.7$, [5] : $T = 0.9$

(in case a) the limit cycles [0], [1]cannot be separated; in case b) there is small disagreement).

Figure 4: Limit cycles of van der Pol's oscillator ($\epsilon = 1.7, x_{0_1} = 0., x_{0_2} = 2$): numerically calculated [0], first order approximation : $\underline{S}_T^{(1)}(\underline{x}_0)$ for several strobe times T: a) [1] : $T = 0.1$, [2] : $T = 0.2$ b) [3] : $T = 0.3$

4 Higher Order Approximations of the Stroboscopic Map

In the last chapter we demonstrated that already in first order approximation typical nonlinear behavior can be reproduced qualitatively. The next question is, what happens if one goes to higher order approximations. Can one derive a good quantitative solution, too, using this algebraic method?
In practice the modes of higher orders cannot be calculated by hand because the higher the order, the larger is the inhomogeneity of the linear differential equations of these modes in Eq.(7). This is the problem for calculating the stroboscopic map to any order. Using algebraic manipulation programs like reduce [27], macsyma [26] few more modes of higher order can be derived. But because the algebraic manipulation programs are based on standard analysis solving methods for linear differential equations, they are not efficient enough to do this to any order. For example with macsyma one is able to get all mode amplitudes to fifth order for the van der Pol oscillator.
Already using this fifth order approximation of van der Pol's oscillator we investigate the algebraic method in more detail.
Remark 4.1: In the case of van der Pol's oscillator we have the additional symmetry property $\underline{f}(-\underline{x}) = -\underline{f}(\underline{x})$. This causes that all modes $a_{j,\underline{m}} \in \mathbf{R}$ of even order vanish. Therefore we investigate the $k-th$ order approximation for $k = 1, 3, 5$.
There exists numerical evidence for the following statements:
Statement 4.1: For a given order $k = 1, 3, 5$ there exists a maximum parameter $\epsilon_{max}^{(k)}$ such, that for all $\epsilon > \epsilon_{max}^{(k)}$ the iteration diverges for all $T > 0$.

$$\underline{S}_{T,\epsilon}^{(k),n}(\underline{x}_0) \overset{n\to\infty}{\to} \infty$$

Here we have used the abbreviation $\underline{S}_T^n := \underline{S}_T^{n-1} \circ \underline{S}_T = \underline{S}_T^{n-1}(\underline{S}_T(\underline{x}_0)), \underline{S}_T^0 := \underline{id}$, n is called number of iterations and k is the order of the Taylor series in the initial values of $\underline{S}_T$.
By numerical investigation we have

k	1	3	5
ϵ_{max}	2[	2[	0.6

for $T > 0$ (whereby T is varyed in steps of $\Delta T = 0.1$) and $0 \leq \epsilon < 2$ (ϵ is variied in steps of $\Delta\epsilon = 0.1$). $\epsilon_{max} = 2[$ corresponds to the unrestricted interval $\epsilon < 2$.
Of course there exists a convergent iteration for $k = 5, T < 0.1$ and $\epsilon > 0.6$, but we investigated this iteration behavior due to convergence by varying ΔT in steps of $\Delta T = 0.1$.
Statement 4.2: For a given order $k \leq k_{max}(= 5)$ and a fixed $\epsilon \leq \epsilon_{max}^{(k)}$ there

exists a maximum stroboscopic time $T^{(k)}_{max,\epsilon}$ to each ϵ with $T^{(k)}_{max,\epsilon} > 0$, such that for $T > T^{(k)}_{max,\epsilon}$ the iteration diverges.

$$\underline{S}^{(k),n}_{T,\epsilon}(\underline{x}_0) \overset{n\to\infty}{\longrightarrow} \infty$$

Fig.(5) shows the results of this numerical investigations (ϵ and T is varied in steps of 0.1).

- For $\epsilon = 0$ is $T^{(k)}_{max,0} = \infty \quad \forall \quad k = 1,3,5$, because in this case Eq.(16) is reduced to the differential equation of the harmonic oscillator.
- For a given order $k = 1,3,5$ we get: the larger ϵ the smaller $T^{(k)}_{max,\epsilon}$ for a converging iteration. This seems understandable, because the algebraic expression for the mode amplitudes and therefore for the stroboscopic map depends on the expression $e^{\epsilon T}$. Therefore the individual modes $\underline{a}_{j,m}$ are increasing with ϵ and T.

Figure 5: Maximum stroboscopic time $T^{(k)}_{max,\epsilon}$ which corresponds to a converging iteration [filled box]and a diverging iteration [unfilled box]for $n = 10^4$ iterations, $x_{0_1} = 0., x_{0_2} = 0.1$ and several orders a) $k = 1$, b) $k = 3$, c) $k = 5$

In addition to Fig.(5) the iteration converges in the case $k = 3$ for a few more special parameter values: For $\epsilon = 0.1$ there is convergence, too for $T \in [6.0, 19.9] \cup \{20.6\}$ and for $\epsilon = 0.2$ when $T \in [6.0, 7.7] \cup \{9.0\}$ Thus in the case of $\epsilon = 0.1$ and $\epsilon = 0.2$ we are able to derive an algebraic expression $\underline{S}^{(3)}_{6.}(\underline{x}_0)$ as the Poincaré map, which reflects the periodic motion as seen in Fig.(6)

Further numerical results involve that the convergence-divergence-behavior does not depend sensitive on the number of iterations. In about $3 \times 20 \times 70$ different used parameter values k, ϵ, T we get only 4 cases in which the iteration converges for $n = 500$ iterations and diverges for $n = 10^4$. This reflects a kind of stability of this algebraic method in long-time-predictions.

What is the best stroboscopic time, for a given $\epsilon \leq \epsilon_{max}^{(k)}, T \leq T_{max,\epsilon}^{(k)}$ to describe the limit cycle behavior using this algebraic integration method?
Definition 4.1: Let $\underline{X}_T(\underline{x}_0) \in \mathbf{R}^2$ be a numerically calculated iteration point of Eq.(16) and $\underline{S}_T^{(k)}(\underline{x}_0) \in \mathbf{R}^2$ a $k-th$ order approximation for the map, then the quantity $< r^{(k)} >$ is defined as the *averaged difference between numerical and algebraic limit cycle.*

$$< r^{(k)} > := \frac{1}{n} \sum_{i=1}^{n} |\underline{S}_T^{(k),i}(\underline{x}_0) - \underline{X}_T(\underline{S}_T^{(k),i-1}(\underline{x}_0))|$$

(Again as defined in statement 4.1 index i corresponds to the i -- th iterate of $\underline{S}_T$) Caused by Comparison of Fig.(7) and (8) we argue that $< r^{(k)} >$ is a possible quantity to describe the agreement of numerical and algebraic results.
As general behavior for $\epsilon \leq \epsilon_{max}^{(k)}, T \leq T_{max,\epsilon}^{(k)}$ and different orders $k = 1, 3, 5$ we derive:

- For $k = 1, 3, 5$: Except for the oscillating effects $< r^{(k)} >$ increases with T which corresponds to a decreasing agreement of numerical and algebraic limit cycles for all calculated orders.
- For $k = 3, 5$: $\frac{d<r^{(1)}>}{dT} > \frac{d<r^{(k)}>}{dT}$. This means that for larger T and higher orders the time dependence of the approximation quality changes slower respectively the algebraic solution seems to be a better approximation for $k = 3, 5$ compared with $k = 1$.
- For $0.3 \leq T < T_{max,\epsilon}^{(k)}$:$< r^{(5)} > << r^{(3)} > << r^{(1)} >$. This seems in agreement with the plots in Fig.(7) that a fifth order map causes a better approximation than a third order and than a first order map.
- For $T = 0.2$ the approximation of $\underline{S}_T$ is for $k = 1$ better than for $k = 3, 5$. Perhaps in this case $< r^{(k)} >$ is too small to derive quantitative predictions.

Nevertheless $< r^{(k)} >$ is an approximative quantity to describe the agreement of numerical and algebraic limit cycle. To derive quantitative predictions $| < r^{(i)} > - < r^{(j)} > |$ should be not too small.

As seen in Fig.(9,10) we obtain this general behavior also for $\epsilon = 0.5$. In this case we observe a kind of resonance in Fig.(10) for the fifth order solution in the interval of $T \in [0.12, 0.31]$ where the iteration of $\underline{S}_T^{(5)}(\underline{x}_0)$ diverges. Currently we do not understand this. Nevertheless we get the best approximation using $\underline{S}_{0.5}^{(5)}(\underline{x}_0)$ as seen by comparison of Fig.(9),(10). In this case there is good agreement between numerical and algebraic limit cycle except 2 places in phase space. A few comments on this will be given in chapt.6.
In the example of van der Pol's oscillator we demonstrated that using approximations of higher than first order for stroboscopic maps a really good quantitative agreement between numerical and algebraic solution can be derived. The observation that for a given $T, \epsilon \in \mathbf{R}$ a higher order approximation do not have to be a better approximation is not a typical effect of this algebraic method: it also corresponds to numerical methods as for example the Runge-Kutta-algorithm where a higher order do not has to involve a higher accuracy to the solution [24].
As numerical results demonstrate, there is no difference whether the numerical iteration point $\underline{X}_T(\underline{x}_0)$ is calculated by a Stör-Bulirsch method or by an Euler integration procedure (step-size = 0.01). Therefore an estimation of the optimal stroboscopic time $T \in \mathbf{R}$ can be derived independend on numerical solving packages.

Figure 6: Periodic motion of van der Pol's oscillator ($\epsilon = 0.2$) : [×] algebraically described by the Poincaré map: $\underline{S}_6^{(3)}(\underline{x}_0)$, as a comparison to the numerically calculated limit cycle [solid line].

Figure 7: Comparison of limit cycles of van der Pol's system ($\epsilon = 0.3$): [0] numerically, [1]algebraic $\underline{S}_T^{(1)}(\underline{x}_0)$, [3]algebraic $\underline{S}_T^{(3)}(\underline{x}_0)$, [5]algebraic $\underline{S}_T^{(5)}(\underline{x}_0)$ for different T. a) $T = 0.2$, b) $T = 0.5$, c) $T = 0.7$

Figure 8: Van der Pol's system ($\epsilon = 0.3$): Averaged difference between numerically and algebraic calculated limit cycle $< r^{(k)} > (T)$ for different orders $k : ([1] : k = 1, [3] : k = 3, [5] : k = 5)$ and $n = 10^3$ iterations.

Figure 9: Comparison of limit cycles of van der Pol's system ($\epsilon = 0.5$): [0] numerically, [1]algebraic $\underline{S}_T^{(1)}(\underline{x}_0)$, [3]algebraic $\underline{S}_T^{(3)}(\underline{x}_0)$, [5]algebraic $\underline{S}_T^{(5)}(\underline{x}_0)$ for different T. a) $T = 0.2$, b) $T = 0.4$, c) $T = 0.5$

Figure 10: Time dependence of $< r^{(k)} >$ for $\epsilon = 0.5$ and given orders $k = 1, 3, 5$, corresponding to $[1], [3], [5]$ and $n = 10^3$ iterations.

5 Estimation of the Rest Term

With a kind of hybrid ansatz we take into account all modes of higher than first order to improve the results of first order approximations of $\underline{S}_T(\underline{x}_0)$.

Definition 5.1: The difference between the exact stroboscopic map $\underline{S}_T(\underline{x}_0) \in \mathbf{R}^n$ (defined by Eq.(3)) and the first order approximation $\underline{S}_T^{(1)}(\underline{x}_0) \in \mathbf{R}^n$ (defined by definition 2.3) is called *rest term* $\underline{\Delta}_T(\underline{x}_0) \in \mathbf{R}^n$:

$$\underline{S}_T(\underline{x}_0) = \underline{S}_T^{(1)}(\underline{x}_0) + \underline{\Delta}_T(\underline{x}_0) \tag{18}$$

In the case of van der Pol's oscillator we demonstrate explicitly that the rest term caused by truncation of the power series in the initial values can be approximated by a differential equation for $\underline{\Delta}_T(\underline{x}_0) \in \mathbf{R}^2$. Inserting Eq.(18) in Eq.(17) leads to this nonlinear differential equation for the components of $\underline{\Delta}_T(\underline{x}_0) \in \mathbf{R}^2$

$$\begin{pmatrix} \dot{\Delta}_1 \\ \dot{\Delta}_2 \end{pmatrix} = \begin{pmatrix} 0 & 1 \\ -(1 + 2\epsilon S_1^{(1)2} S_2^{(1)}) & \epsilon(1 - S_1^{(1)2}) \end{pmatrix} \begin{pmatrix} \Delta_1 \\ \Delta_2 \end{pmatrix} + \underline{\Xi}(\underline{x}_0, T) + \underline{\Phi}(\underline{x}_0, T) \tag{19}$$

$\underline{\Xi}(\underline{x}_0, T) \in \mathbf{R}^2$ is the nonlinear part of the differential equation:

$$\underline{\Xi}(\underline{x}_0, T) = -\epsilon \begin{pmatrix} 0 \\ S_2^{(1)} \Delta_1^2 + 2 S_1^{(1)} \Delta_1 \Delta_2 + \Delta_1^2 \Delta_2 \end{pmatrix} \tag{20}$$

$\underline{\Phi}(\underline{x}_0, T) \in \mathbf{R}^2$ is the inhomogeneity of the equation:

$$\underline{\Phi}(\underline{x}_0, T) = \begin{pmatrix} 0 \\ -\epsilon S_1^{(1)2} S_2^{(1)} + \epsilon x_{0_1}^2 x_{0_2} (a_{1,10}^2 a_{2,01} + 2 a_{1,10} a_{1,01} a_{2,10}) \end{pmatrix} \tag{21}$$

As initial condition we get from the identity Eq.(5, 18)

$$\Delta_{1,0}(\underline{x}_0) = \Delta_{2,0}(\underline{x}_0) = 0 \tag{22}$$

With the use of $\Delta_1 =: \Delta$ and after linearizing Eq. (19) we obtain an autonomous differential equation of the form

$$\ddot{\Delta} + c_1(\underline{x}_0, T)\dot{\Delta} + c_2(\underline{x}_0, T)\Delta = \Phi_2(\underline{x}_0, T) \tag{23}$$

where $c_1, c_2, \Phi_2 \in \mathbf{R}$ depend on $\underline{x}_0$, but also on T in a complicated way.
Note that $\underline{\Delta}_T$ corresponds to the linearized rest term in the following.
In a general case the time dependence of the coefficients $c_1(\underline{x}_0, T)$ and $c_2(\underline{x}_0, T)$ involves that Eq.(23) cannot be solved analytically. Therefore as a first approximation we integrate Eq.(23) by a numerical solving method [24]. After each iteration step this linearized rest term $\underline{\Delta}_T(\underline{x}_0)$ is added to the first order approximation $\underline{S}_T^{(1)}(\underline{x}_0)$ of the stroboscopic map.

This correction causes additional good quantitative agreement of algebraic and numerical limit cycles as Fig.(11) demonstrates.

Figure 11: Limit cycles of van der Pol's oscillator ($\epsilon = 0.3$) for different approximation methods: [0] :numerically, [1]:algebraic first order approximation: $\underline{S}_{0.5}^{(1)}(\underline{x}_0)$, [2]:using numerically calculated rest term: $\underline{S}_{0.5}^{(1)}(\underline{x}_0) + \underline{\Delta}_{0.5}(\underline{x}_0)$

In this approximation we cannot neglect numerical solving methods. Thus to be independent of numerical algorithms we replace in the coefficients $c_1(\underline{x}_0, T), c_2(\underline{x}_0, T)$ and the inhomogeneity $\Phi_2(\underline{x}_0, T)$ of Eq.(23) T by an effective stroboscopic time T_{eff} as a further approximation.

$$c_1(\underline{x}_0, T) \rightarrow \tilde{c}_1(\underline{x}_0, T_{eff}), c_2(\underline{x}_0, T) \rightarrow \tilde{c}_2(\underline{x}_0, T_{eff}), \Phi_2(\underline{x}_0, T) \rightarrow \tilde{\Phi}_2(\underline{x}_0, T_{eff})$$

For convenience $' \sim '$ is neglected in the following.
This replacements involve that Eq.(23) becomes a linear differential equation with constant coefficients and the form of a driven harmonic oscillator.

$$\ddot{\Delta} + c_1(\underline{x}_0, T_{eff})\dot{\Delta} + c_2(\underline{x}_0, T_{eff})\Delta = \Phi_2(\underline{x}_0, T_{eff}) \tag{24}$$

This equation can be soived analytically

$$\Delta_T(\underline{x}_0, T_{eff}) = \frac{\Phi_2}{c_2}\left(\frac{D^-}{D^+ - D^-}e^{D^+T} + \frac{D^+}{D^- - D^+}e^{D^-T} + 1\right) \tag{25}$$

with $D_{\pm} = -\frac{c_1}{2} \pm \frac{1}{2}\sqrt{c_1^2 - 4c_2}$.
Thus in this last approximation of the rest term, the map $\underline{S}_T \in \mathbf{R}^2$ can be written as

$$\underline{S}_T(\underline{x}_0, T_{eff}) = \underline{S}_T^{(1)}(\underline{x}_0) + \begin{pmatrix} \Delta_T(\underline{x}_0, T_{eff}) \\ \dot{\Delta}(\underline{x}_0, T_{eff}) \end{pmatrix} \tag{26}$$

T_{eff} appears as an additional parameter in Eq.(26), which can be chosen such way, that we get best agreement in numerical and algebraic calculated limit cycles. Fig.(12) demonstrates that a variation of the parameter T_{eff} corresponds to a variation of the size of the limit cycle. Therefore the best parameter value of T_{eff} (in the sense of best agreement) can be fig d out as $T_{eff} = 0.3$.
In the following we describe the mathematical determination of the bes T_{eff}.
Definition 5.2: Let $\underline{x}^A := \underline{S}_T(\underline{x}_0, T_{eff})$ be an algebraic calculated iteration point of Eq.(26) and $\underline{x}^N = \underline{X}_T(\underline{x}_0)$ be a numerically calculated iteration point [24]: then the quantity $r := |\underline{x}^A - \underline{x}^N|$ depending on T_{eff} describes the *difference of numerical and algebraic solution.*
We argue that the minimum value of r as a function of T_{eff} corresponds to this parameter value of T_{eff} with best agreement in numerical and algebraic solution. Compare Fig. (12) and (13).
Again there is no difference if $\underline{x}^N$ is calculated by an Euler method (step-size = 0.01) or by a Stör-Bulirsch method [24]. This important feature involves the independence of the determination of the best T_{eff} on numerical solving packages for ODE' s.

We have done analogous calculations with Rőssler's system [18]:

$$\begin{pmatrix} \dot{x} \\ \dot{y} \\ \dot{z} \end{pmatrix} = \begin{pmatrix} 0 & -1 & -1 \\ 0 & 0.2 & 0 \\ 0 & 0 & -\mu \end{pmatrix} \begin{pmatrix} x \\ y \\ z \end{pmatrix} + \begin{pmatrix} 0 \\ 0 \\ b + xz \end{pmatrix} \tag{27}$$

$b, \mu \in \mathbf{R}$
By the introduction of the parameter b as an additional variable, with $b(0) = b$, the origin is fixed point of the transformed system of the ODE

$$\begin{pmatrix} \dot{x} \\ \dot{y} \\ \dot{z} \\ \dot{b} \end{pmatrix} = \begin{pmatrix} 0 & -1 & -1 & 0 \\ 0 & 0.2 & 0 & 0 \\ 0 & 0 & -\mu & 1 \\ 0 & 0 & 0 & 0 \end{pmatrix} \begin{pmatrix} x \\ y \\ z \\ b \end{pmatrix} + \begin{pmatrix} 0 \\ 0 \\ xz \\ 0 \end{pmatrix} \tag{28}$$

In Fig. (14) and (15) we compare numerical results (a) with algebraic ones for periodic and chaotic behavior, which depends on the parameter $\mu \in \mathbf{R}$. We demonstrate (b,c), that even for chaotic behavior the qualitative system behavior can be reproduced in low order approximations. In consideration of the rest term (d), which is calculated from the linearized differential equation of the rest term $\underline{\Delta}_T(\underline{x}_0)$ the algebraic iteration points are lying on the numerically calculated phase trajectories.

In the case of Rössler's system we integrated the linearized rest term $\underline{\Delta}_T(\underline{x}_0) \in \mathbf{R}^4$ numerically [24]. In principle the time dependence of the coefficients in the differential equation of the rest term can be approximated by an effective time step T_{eff}, as it is done explicitly in the case of van der Pol's system. To solve this resulting differential equation with constant coefficients one have to find out the zero-points of the characteristic polynomial, which is of third order. In the case of Rössler's system this expression for the zero-points is so complicated, that we could not apply the second kind of approximation of the rest term, yet.

Figure 12: Variation of T_{eff} causes variation of the size of the limit cycles of van der Pol's oscillator ($\epsilon = 0.3$): numerically [0] and algebraic, using $\underline{S}^{(1)}_{0.5}(\underline{x}_0) + \underline{\Delta}_{0.5}(\underline{x}_0, T_{eff})$ for [1]$T_{eff} = 0.1$, [2]$T_{eff} = 0.2$, [3]$T_{eff} = 0.3$, [4]$T_{eff} = 0.4$, [5]$T_{eff} = 0.5$

Figure 13: Determination of best T_{eff} for the rest term approximation in the case of van der Pol's system ($\epsilon = 0.3, T = 0.5$)

Figure 14: Periodic behavior of Rössler's system ($\mu = 1.5, \underline{x}_0 = (1, 0, 1)$): [0] : numerically, [1] : first order approximation: $\underline{S}^{(1)}_{0.1}(\underline{x}_0)$, [2] : second order approximation $\underline{S}^{(2)}_{0.1}(\underline{x}_0)$, [3] : using $\underline{S}^{(1)}_{0.1}(\underline{x}_0) + \underline{\Delta}_{0.1}(\underline{x}_0)$, where $\underline{\Delta}_T \in \mathbf{R}^4$ is the linearized rest term, numerically calculated.

Figure 15: Chaotic behavior of Rössler's system ($\mu = 5.7, \underline{x}_0 = (1, 0, 1)$), whereby the transient response is not neglected: a) numerically, b) first order approximation: $\underline{S}^{(1)}_{0.1}(\underline{x}_0)$ c) second order approximation $\underline{S}^{(2)}_{0.1}(\underline{x}_0)$ d) using $\underline{S}^{(1)}_{0.1}(\underline{x}_0) + \underline{\Delta}_{0.1}(\underline{x}_0)$, where $\underline{\Delta}_T \in \mathbf{R}^4$ is the linearized rest term, numerically calculated.

6 Correlation of the Algebraic Method with the Local Divergence Rate of a Dynamical System

Definition 6.1: Let $\underline{S}_T(\underline{x}_0) = \underline{x}(T) \in \mathbf{R}^n$ be the stroboscopic map as defined in Eq.(3) then

$$\underline{S}_{T_1+T_2}(\underline{x}_0) = \underline{S}_{T_2}(\underline{S}_{T_1}(\underline{x}_0)) \tag{29}$$

is called *semi group condition.*

Lemma 6.1: Let $\underline{S}_T \in \mathbf{R}^n$ be given as a power series in the initial values $\underline{x}_0$ of the system, like Eq.(6), then Eq.(29) is satisfied exactly only if $\underline{S}_T$ is linear in the components of $\underline{x}_0$ or $\underline{S}_T$ is given as an infinite power series.

proof: Inserting Eq.(6) in Eq.(29).

Therefore we make the following definition:

Definition 6.2: For a stroboscopic map $\underline{S}_T(\underline{x}_0) \in \mathbf{R}^n, \delta_{semi} \in \mathbf{R}_0^+$ is called *semi group violation*, for

$$\delta_{semi} = |\underline{S}_{T_1+T_2}(\underline{x}_0) - \underline{S}_{T_2}(\underline{S}_{T_1}(\underline{x}_0))| \tag{30}$$

Lemma 6.2: $\delta_{semi} = 0$ for linear differential equations ($\|\underline{l}\|_1 \leq 1$).

proof: The basis for this proof is the known statement: The solution of linear differential equations is always linear in the initial values.(this can also be derived from Eq.(7, 8) proceeding a linear differential equation ($\|\underline{l}\|_1 \leq 1$)).

As demonstrated in chapt.2, the solution of nonlinear systems can be represented as an infinite power series in the initial values. But in reality only a finite number of coefficients $a_{j,\underline{m}}(T) \in \mathbf{R}$ can be calculated. This is the reason why the semi group condition is only satisfied approximatively respectively $\delta_{semi} > 0$ for nonlinear systems. Of course δ_{semi} depends on the several kinds respectively orders of approximations of the stroboscopic map $\underline{S}_T \in \mathbf{R}^n$, demonstrated in chapt.(2-5).

In the case of van der Pol's oscillator we demonstrate the mutual dependency of the semi-group-violation δ_{semi}, the local divergence rate λ_{loc} of the physical system and the agreement between numerically and algebraic calculated limit cycle.

The local divergence rate describes how fast nearby trajectories separate locally and is defined in [30].

$$\lambda_{loc,i}(x) = \frac{1}{2} * Eigenvalue[D_x\underline{f} + D_x\underline{f}^{tr}] \quad \text{and} \quad \underline{x} \in \mathbf{R}^n \tag{31}$$

For the van der Pol oscillator Eq.(16) leads to

$$\lambda_{loc_{1,2}}(x) = \frac{\epsilon}{2}[(1-x^2) \pm \sqrt{(1-x^2)^2 + 4x^2y^2}] \tag{32}$$

In Fig.(16) there δ_{semi} and $\lambda_{loc} := max\{\lambda_{loc_1}, \lambda_{loc_2}\}$ is plotted for each point of the limit cycle. At this 2 edges of the limit cycle, where the difference between numerical and algebraic solution is maximal, there a nonvanishing δ_{semi} is related to a nearly vanishing local divergence rate.
So it seems: For a given integration time $0 < T \leq T_{max}$ a vanishing local divergence rate amplifies the difference between numerical and algebraic solution whereby a nonvanishing local divergence rate reduces the error. In other words: the place on the limit cycle where δ_{semi} is maximal does not correspond to the maximum difference between numerical and algebraic solution.
Perhaps we can explain by this the property, seen in Fig.(3.4). By enlarging the strobe time $T > 0$ we get typically this maximum disagreement in numerically and algebraic calculated limit cycle at this two edges in the form of sharp peaks.
Fig.(17) and (18) demonstrate, that going to higher order approximations respectively using the linearized rest term as a correction of $\underline{S}_T^{(1)}(\underline{x}_0)$, δ_{semi} can be reduced (for the same parameter values). This involves a better approximation for the limit cycle at places in phase space where the local divergence rate vanishes.

Figure 16: Van der Pol oscillator ($\epsilon = 0.5$): [1]local divergence rate λ_{loc} , [2]semi group violation δ_{semi} and difference between numerically [0] and algebraic $\underline{S}_{0.5}^{(1)}(\underline{x}_0)$[3] calculated limit cycle are correlated.

Figure 17: Van der Pol oscillator ($\epsilon = 0.5$): [0] numerical limit cycle, [3] fifth order algebraic limit cycle: $\underline{S}^{(5)}_{0.5}(\underline{x}_0)$, [1]$\lambda_{loc}$, [2]$\delta_{semi}$

Figure 18: Van der Pol oscillator ($\epsilon = 0.5$): [0] numerical limit cycle, [3] algebraic limit cycle: $\underline{S}^{(1)}_{0.5}(\underline{x}_0) + \underline{\Delta}_{0.5}(\underline{x}_0, 0.3)$, [1]local divergence rate λ_{loc} and [2]δ_{semi}

7 Conclusion

In typical cases dynamical systems which should model physical system behavior describe the experimentally found behavior not exactly. Often some additional, for example not known terms are neglected in the model. Then it seems sufficient to simulate for instance the topological structure of dynamical systems respectively qualitative dynamical effects. In this sense the main interest in this paper was not to derive extremely quantitative agreement between algebraic and numerical solving routines. This question should be answered by choosing really small integration time ($T < 0.1$). But it should be demonstrated that even for not necessarily small strobe times T an algebraic expression is derivable, which describes the dynamical system in a finite, but not infinitesimal neighborhood of the initial state.
The advantage of algebraic integration procedures is, that the whole parameter dependence of the stroboscopic map related to the parameters of the ODE is given in closed form. Therefore the investigation of dynamical system behavior as a function of these parameters is facilitated [23]. Since nonlinear systems tend to have many parameters, a systematic numerical investigation of the solution of the ODE on the parameters seems impossible. The algorithm presented in this paper is closely related to a straight forward algebraic integration by Euler's method. If all the transformations of the resulting algebraic formula are done in order to spare computation time an evaluation using this algebraic formula is quicker than for example Runge-Kutta's algorithm [25].
As Lorenz observed [29], chaotic behavior sometimes occurs when difference equations used as approximations to ODE are solved numerically with an excessively large time increment T. Fig.(19) demonstrates that this computational route to chaos can also appear for some special parameter values for van der Pol's oscillator by iterating the algebraic stroboscopic map. To describe this transition we calculated the largest Ljapunov exponent λ as a function of strobe time T and got following results: $a)T = 11, \lambda = -0.59 b)T = 13, \lambda = -0.38 c)T = 15, \lambda = 0.22 d)T = 16, \lambda = 0.07 e)T = 16.5, \lambda = 0.46 f)T = 18, \lambda = 0.43$. But it turnsed out that also for $T < 11$ there exists $\lambda > 0$ in cases where the limit cycle approximation is very good. Therefore in this case the maximum Ljapunov exponent λ is not a proper quantity to classify this route to computational chaos. For further discussion the paper of Lorenz [29] is a motivation for more detailed investigation of the correspondence of computational chaos and algebraic integration method as a comparison to other solving routines of ODEs.
A generalization of the presented method to ODEs where the flow vector field is just assumed to be an analytic function seems to be straight for-

ward, if the flow vector field is approximated by a polynomial. Discrete maps can be much more easily extracted from experimental systems [11,31] than ODEs. Since the equations of motion of many physical systems are ODEs it is essential to know the stroboscopic map in a closed form in order to make a quantitative comparison between experiment and theory. The application of stroboscopic maps to controlling experimental systems [28] may have important consequences.

Figure 19: Demonstration of the computational route to chaos for large strobe times T of van der Pol's oscillator ($k = 3, \epsilon = 0.1, x_{0_1} = 0, x_{0_2} = .1$): a) $T = 11$, b) $T = 13$, c) $T = 15$, d) $T = 16$, e) $T = 16.5$, f) $T = 18$

ACKNOWLEDGEMENTS

Thanks to W. Eberl for interesting discussions and to the Center for Nonlinear Systems of LANL for the really nice time in Los Alamos and the possibility to do parts of this research there. Also to the Institut E13 at the Technical University of Munich for supporting this work.

References

[1] H.Helmholtz, *Die Lehre von den Tonempfindungen* (Vieweg,1870)

[2] B.van der Pol, *Forced Oscillatons in a Circuit with Nonlinear Resistance* (London, Phil.Mag. **3**,65,1927)
reprinted in: R.Bellman,R.Kalaba,(eds), *Selected Papers on Mathematical Trends on Control Theory* (Dover:New York,1964)

[3] P.Collet,J.P.Eckmann, *Iterated Maps on the Interval as Dynamical Systems* (Birkhäuser,1980)

[4] J.Guckenheimer,P.Holmes, *Nonlinear Oscillations,Dynamical Systems and Bifurcation of Vector Fields* (Springer, New York,1983)

[5] M.Kuchler, W.Eberl, A.Hübler, E.Lüscher, *The Description of Complex Dynamical Systems by Simple Maps* (H.P.A. **61**,232,1988)

[6] A.Wandelt, W.Eberl, A.Hübler, E.Lüscher, *Transformation to Normal Time for the Calculation of Poincaré Maps in a Closed Form* (H.P.A. **62**,1989)

[7] A.Nayveh, D.Mook, *Nonlinear Oscillations* (John Wiley, New York, 1979)

[8] W.Eberl, M.Kuchler, A.Hübler, E.Lüscher, M.Maurer, P.Meinke, *Analytical Representation of Stroboscopic Maps of Ordinary Nonlinear Differential Equations* (Z.Phys.B-Condensed Matter **68**,253,1987)

[9] R. Wackerbauer, W.Eberl, A.Hübler, E.Lüscher, *Analytical Representation of Stroboscopic Maps of Ordinary Nonlinear Differential Equations* (H.P.A. **61**, 236,1988)

[10] M.Berz, *Differential Algebraic Treatment of Beam Dynamics to Very High Orders Including Applications to Space Charge* (preprint,1988)

[11] H.L.Swinney, *Observations of Order and Chaos in Nonlinear Systems* (Physica **7D**,3,1983)

[12] M.J.Feigenbaum, *Universal Behavior in Nonlinear Systems* (Physica **7D**,16,1983)

[13] Mandelbrot, *The Fractal Geometry of Nature* (Freeman,San Francisco,1983)

[14] H.-O. Peitgen, P.H.Richter, *The Beauty of Fractals* (Springer, New York, 1986)

[15] G.Mayer-Kress, H.Haken, *An Explicit Construction of a Class of Suspension and Autonomous Differential Equations for Diffeomorphisms in the Plane* (Commun.Math.Phys **111**,63,1987)

[16] G.Mayer-Kress, *Zur Persistenz von Chaos und Ordnung in nichtlinearen, dynamischen Systemen* (Ph.D.thesis, University of Stuttgart, 1984)

[17] E.N.Lorenz, *Deterministic Nonperiodic Flow* (J.Atmos.Sci **20**,130,1963)

[18] O.E.Rössler, *An Equation for Continuous Chaos* (Phys.Lett. **57A**,397,1976)

[19] A.A.Andronow, A.A.Witt, S.E.Chaikin, *Theorie der Schwingungen* (Akademieverlag,Berlin,1965,chapt.5.1)

[20] I.N.Bronstein,K.A.Semendjajew, *Taschenbuch der Mathematik* (Verlag Harry Deutsch,Frankfurt/Main,1978) p422ff

[21] R.Wackerbauer, *Thesis for Diploma* (Technical University of Munich,1988)

[22] O.Forster, *Analysis 2* (Vieweg,Braunschweig,1981)

[23] W.Eberl, R.Wackerbauer, A.Hübler, *Bifurcation sets of Helmholtz's oscillator* (16mm film)

[24] W.H.Press, B.P.Flannery, S.A.Teukolsky, W.T.Vetterling, *Numerical Recipes* (Cambridge University Press, Cambridge,1988, chapt. 15)

[25] program [illegible] 7500 Bellaire Boulevard, Houston,Texas [illegible]

[26] L.Harten, *Introductory Macsyma* (Paridigm Associates, Inc. for Lawrence Livermore National Laboratory,1987)

[27] A.C.Hearn, *Reduce-Users-Manual* (Rand Publication CP **78**, Santa Monica, 1983)

[28] E.Lüscher, A.Hübler, *Resonant Stimulation of Complex Systems* (H.P.A. **62**,1989)

[29] E.N.Lorenz, *Computational Chaos - Prelude to Computational Instability* (Physica **35D**,299,1989)

[30] J.S.Nicolis, G.Mayer-Kress, G.Haubs, *Non-Uniform Chaotic Dynamics with Implications to Information Processing* (Z.Naturforsch. **38A**,1157-1169,1983)

[31] A.Chao, D.Johnson, et al, *Experimental Investigation of Nonlinear Dynamics in the Fermilab Tevatron*

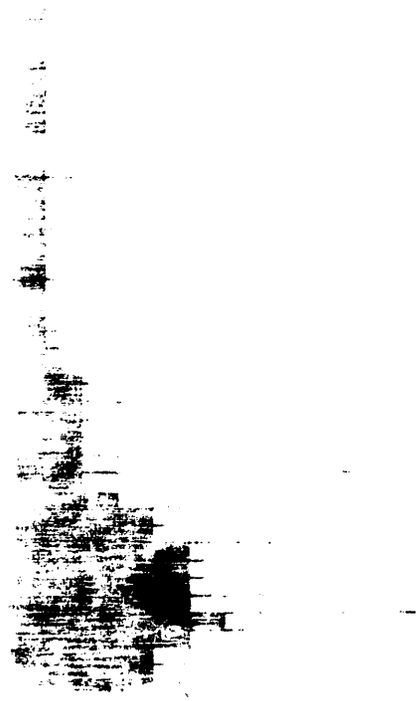

Fig. 1

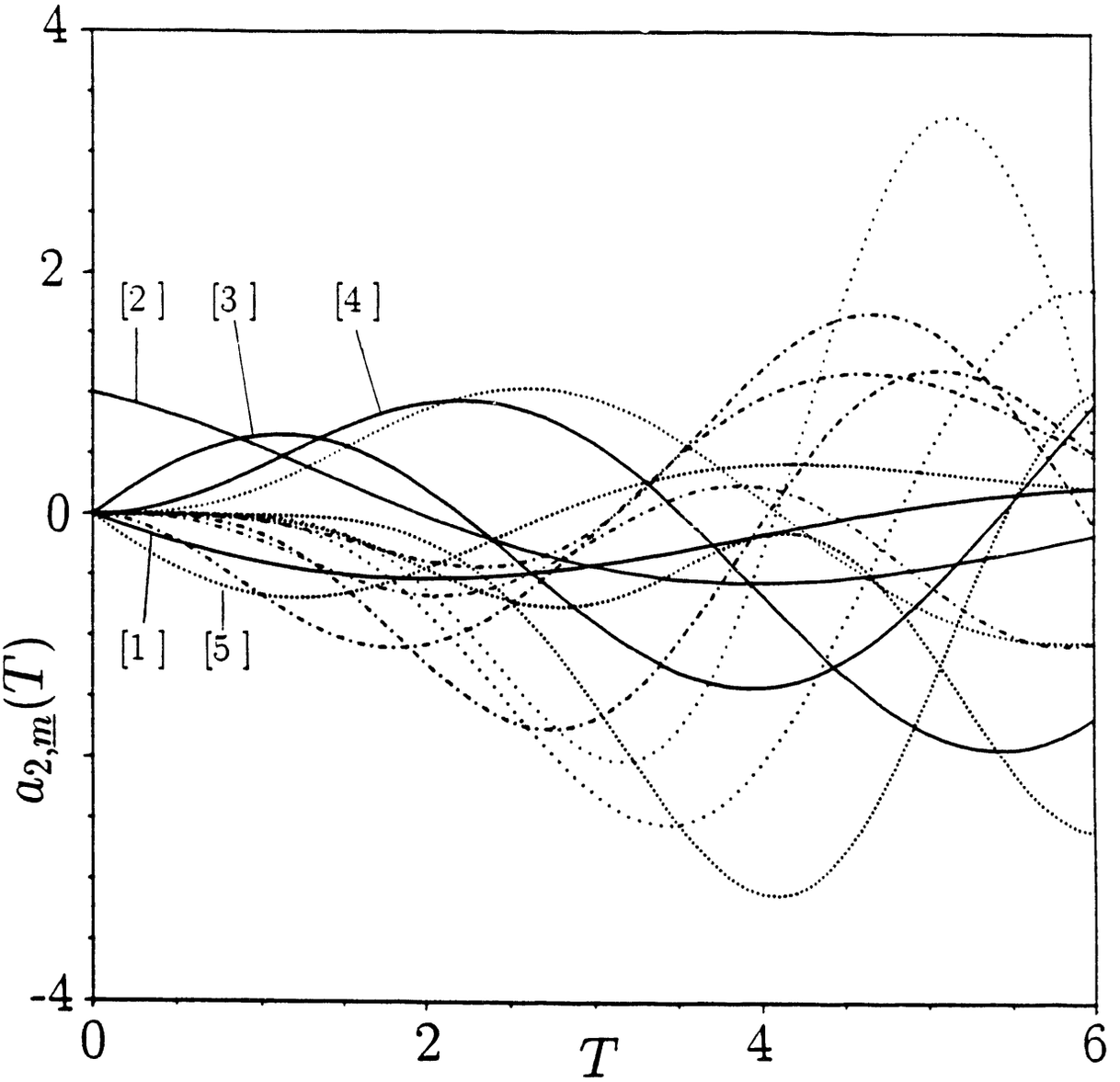

fig. 2a

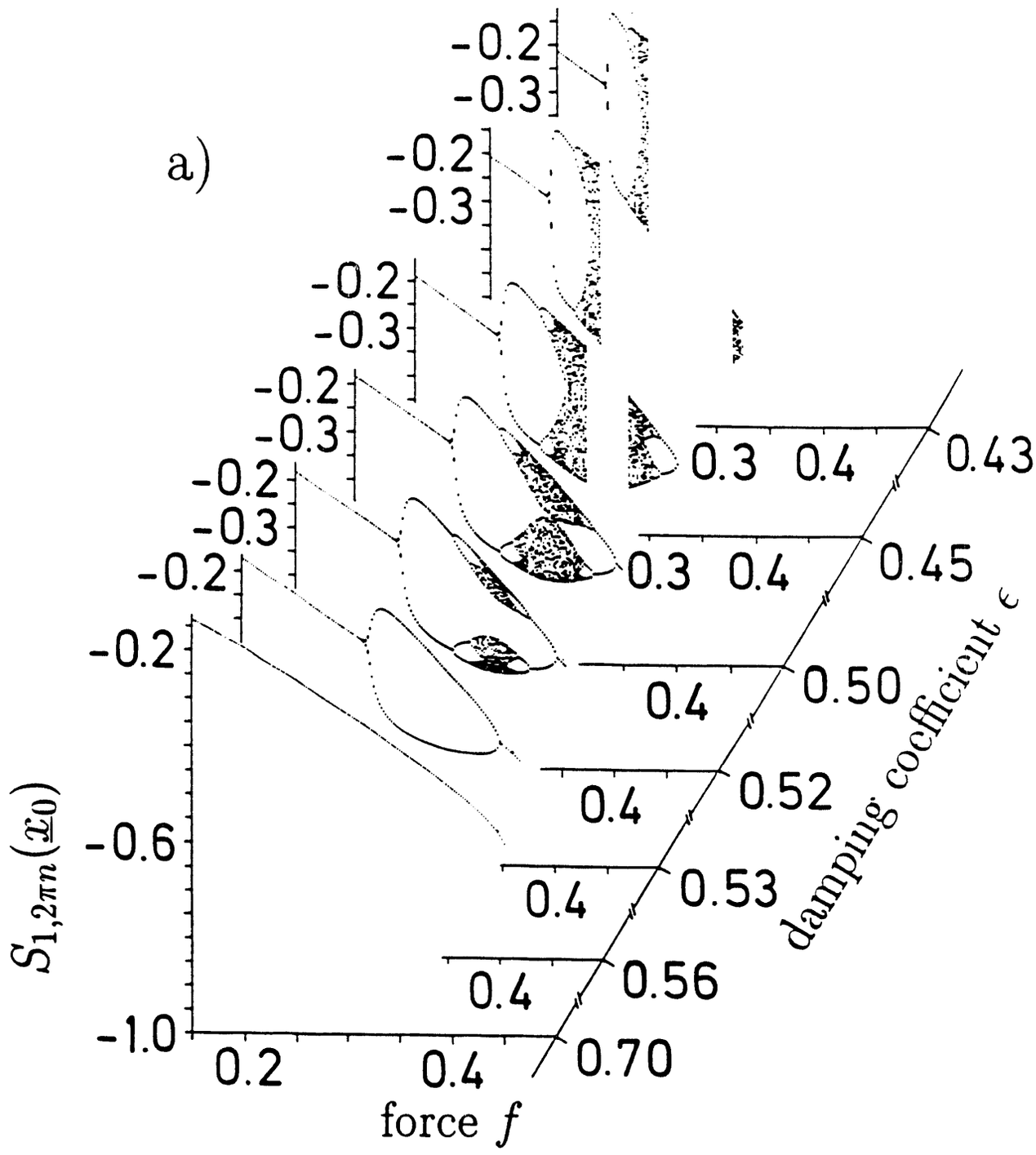
a)
-0.2
-0.3
-0.2
-0.3
-0.2
-0.3
-0.2
-0.3
-0.2
-0.2
-0.6
-1.0
$S_{1,2\pi n}(x_0)$
0.2
0.4
force f
0.3
0.4
0.43
0.3
0.4
0.45
0.4
0.50
0.4
0.52
0.4
0.53
0.4
0.56
0.70
damping coefficient ϵ

Fig 2b

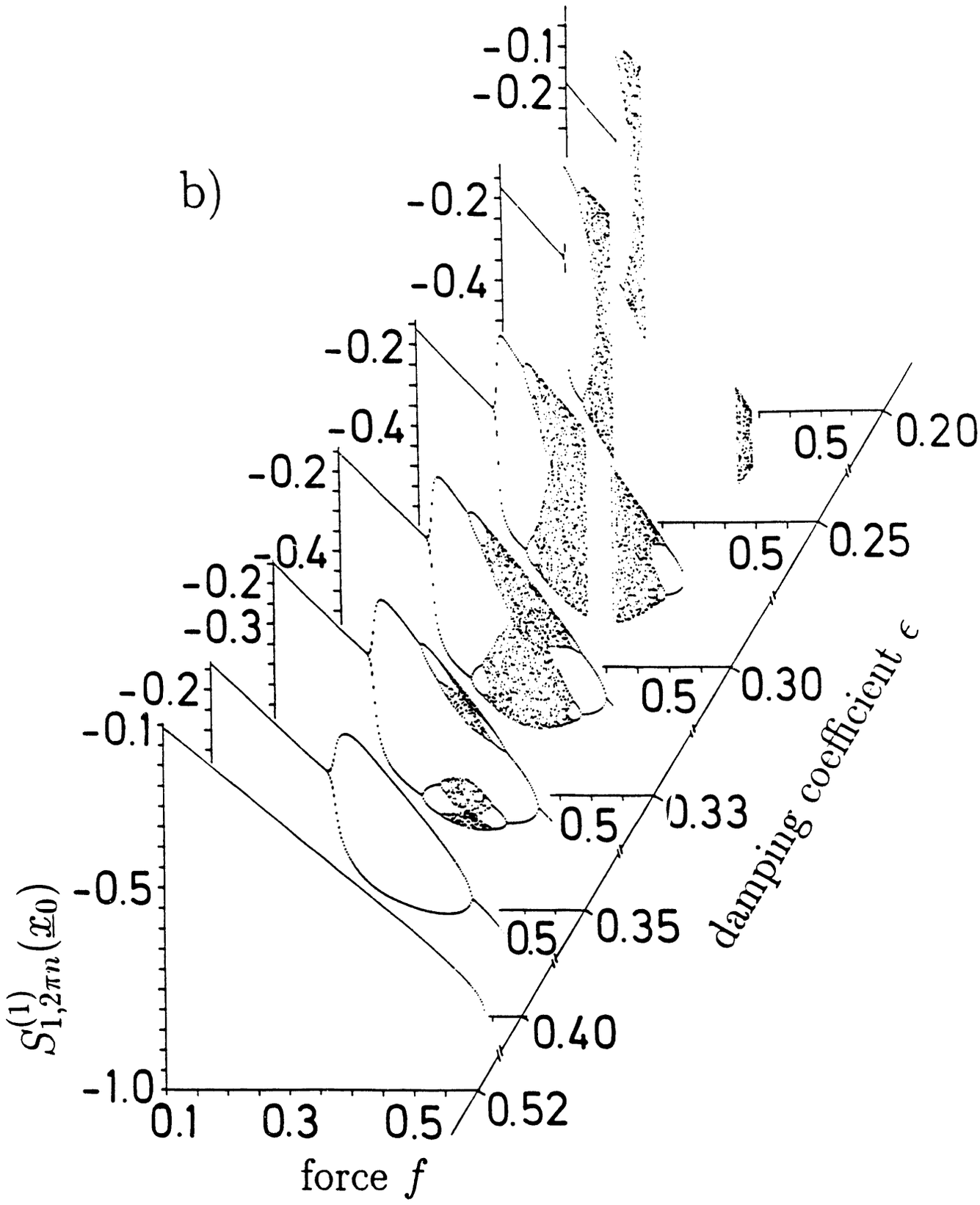
b)
-0.1
-0.2
-0.2
-0.4
-0.2
-0.4
-0.2
-0.4
-0.2
-0.3
-0.2
-0.1
-0.5
-1.0
0.1
0.3
0.5
force f
$S^{(1)}_{1,2\pi n}(\underline{x}_0)$
0.5
0.20
0.5
0.25
0.5
0.30
0.5
0.33
0.5
0.35
0.40
0.52
damping coefficient ϵ

Fig 3a

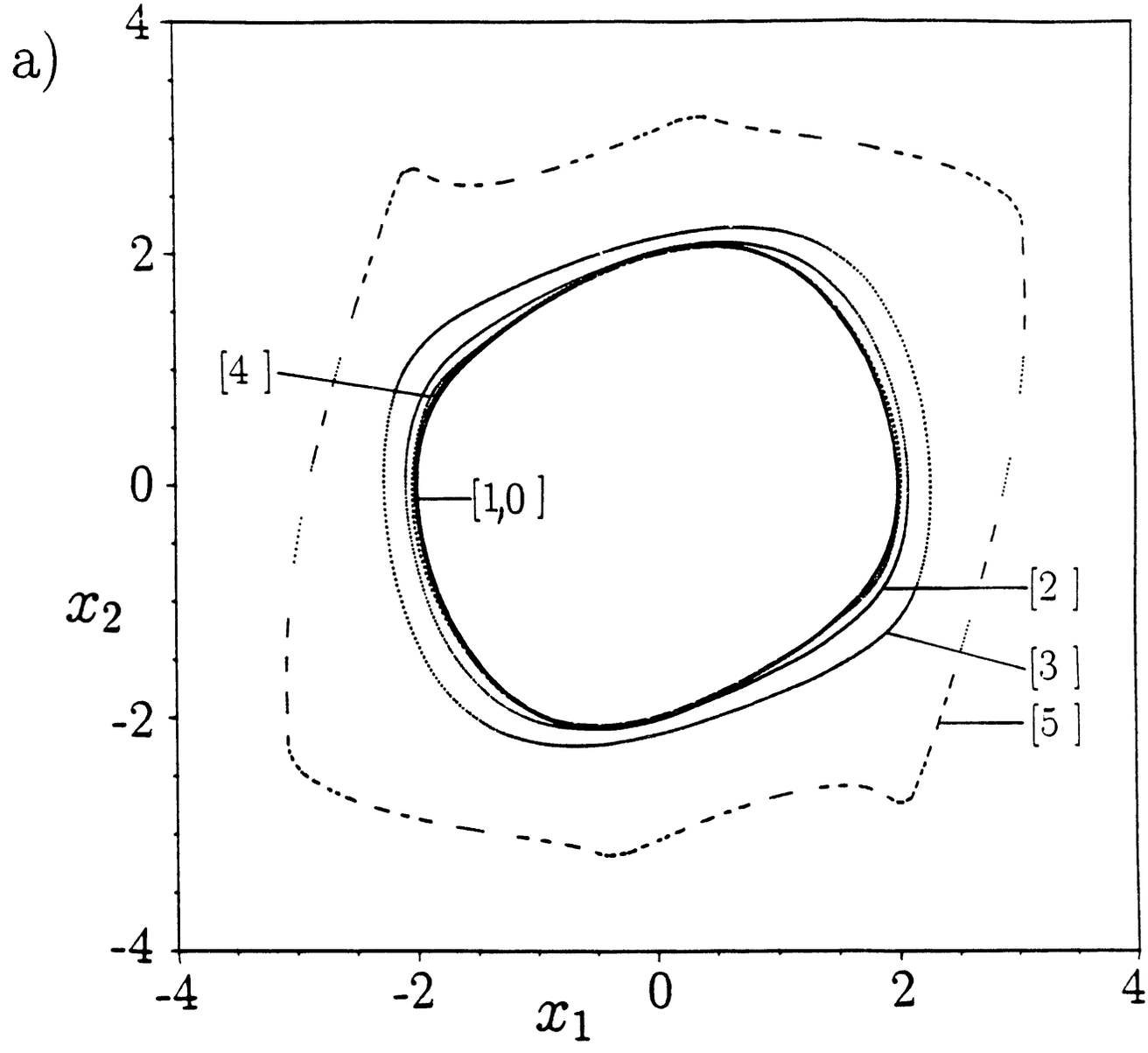

Fig 3b

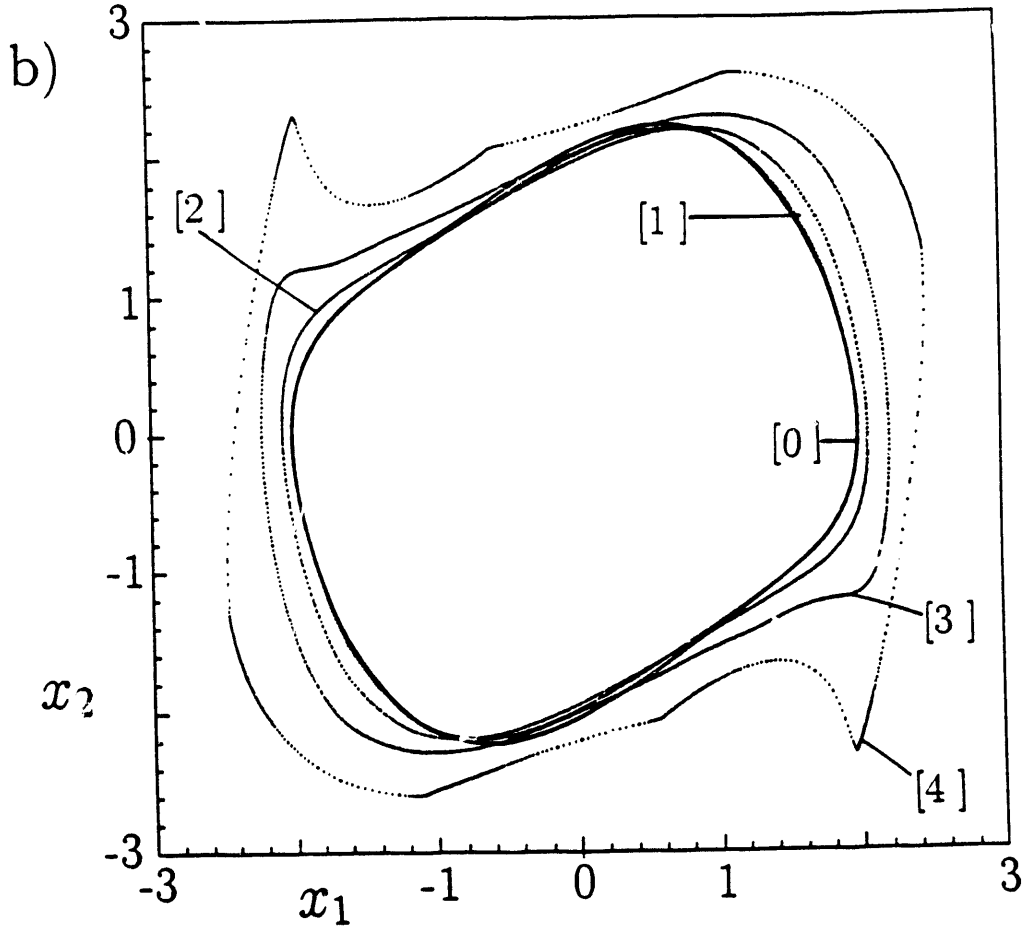

Fig 4a

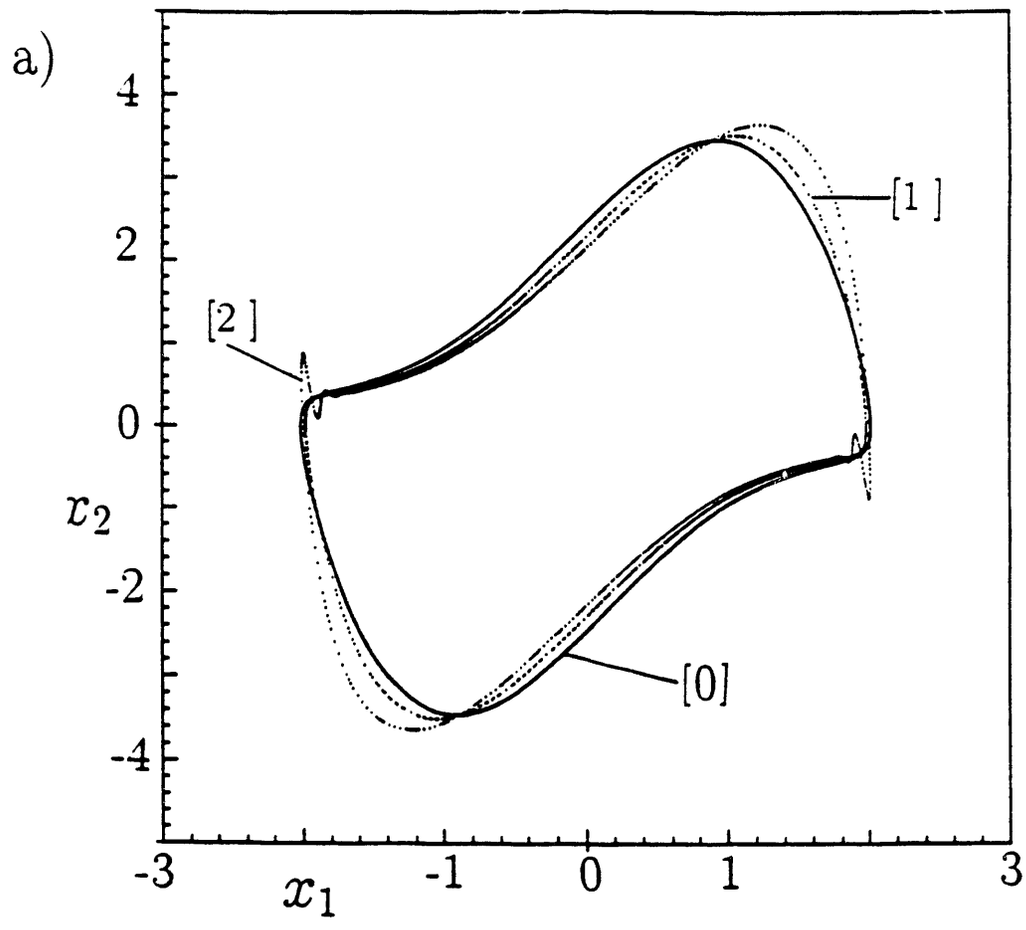

Fig 4b

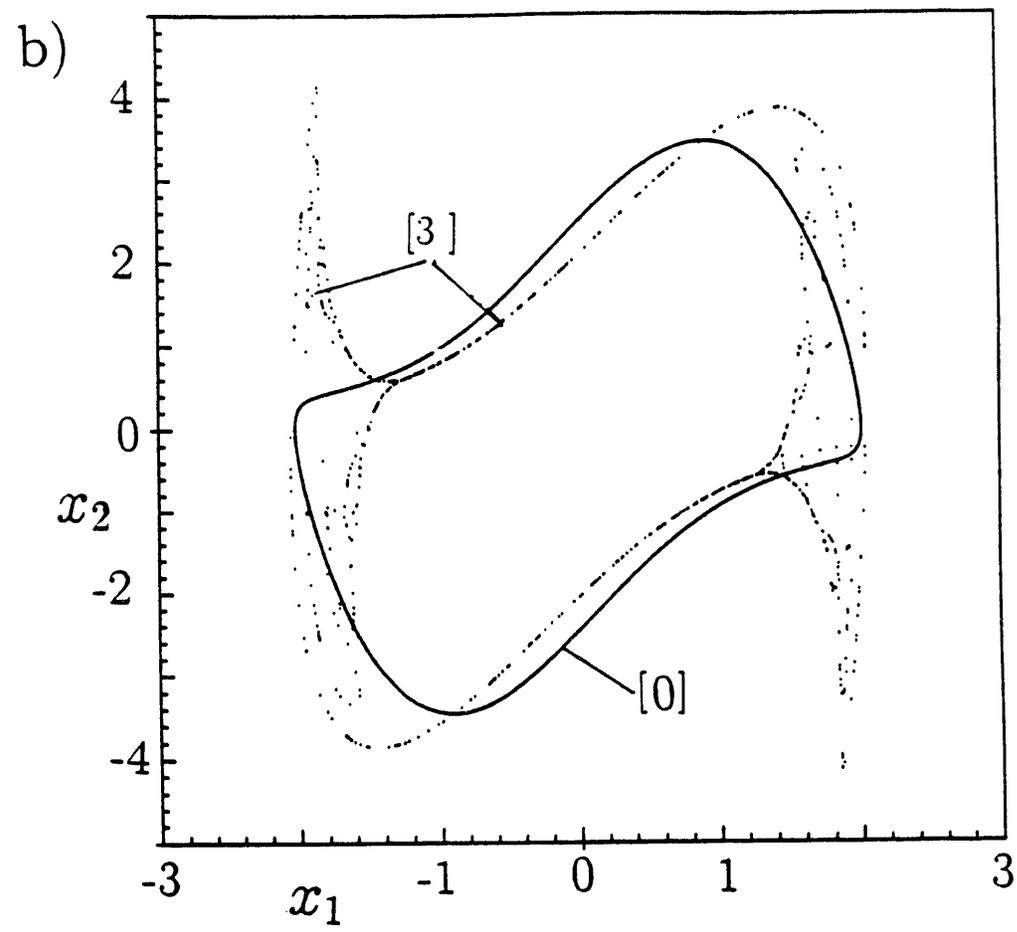

Fig. 5a

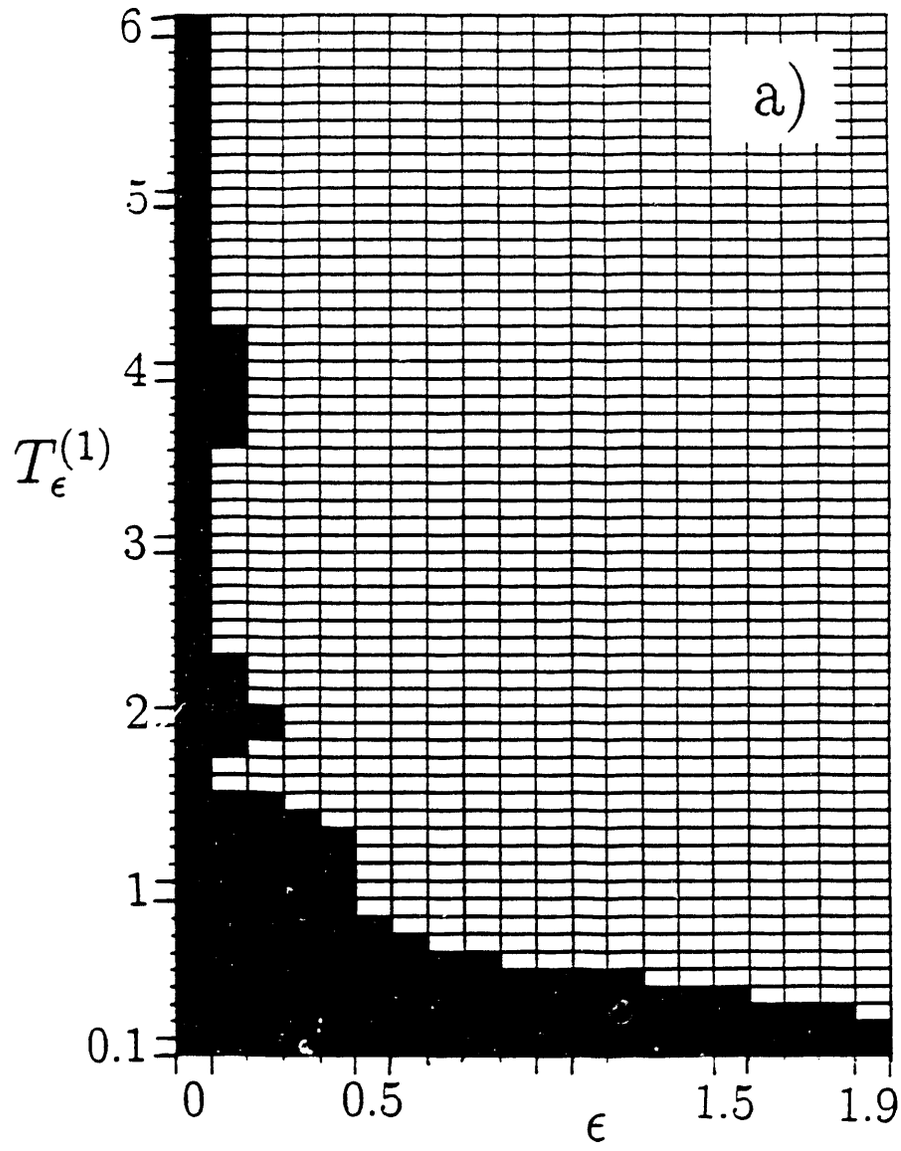

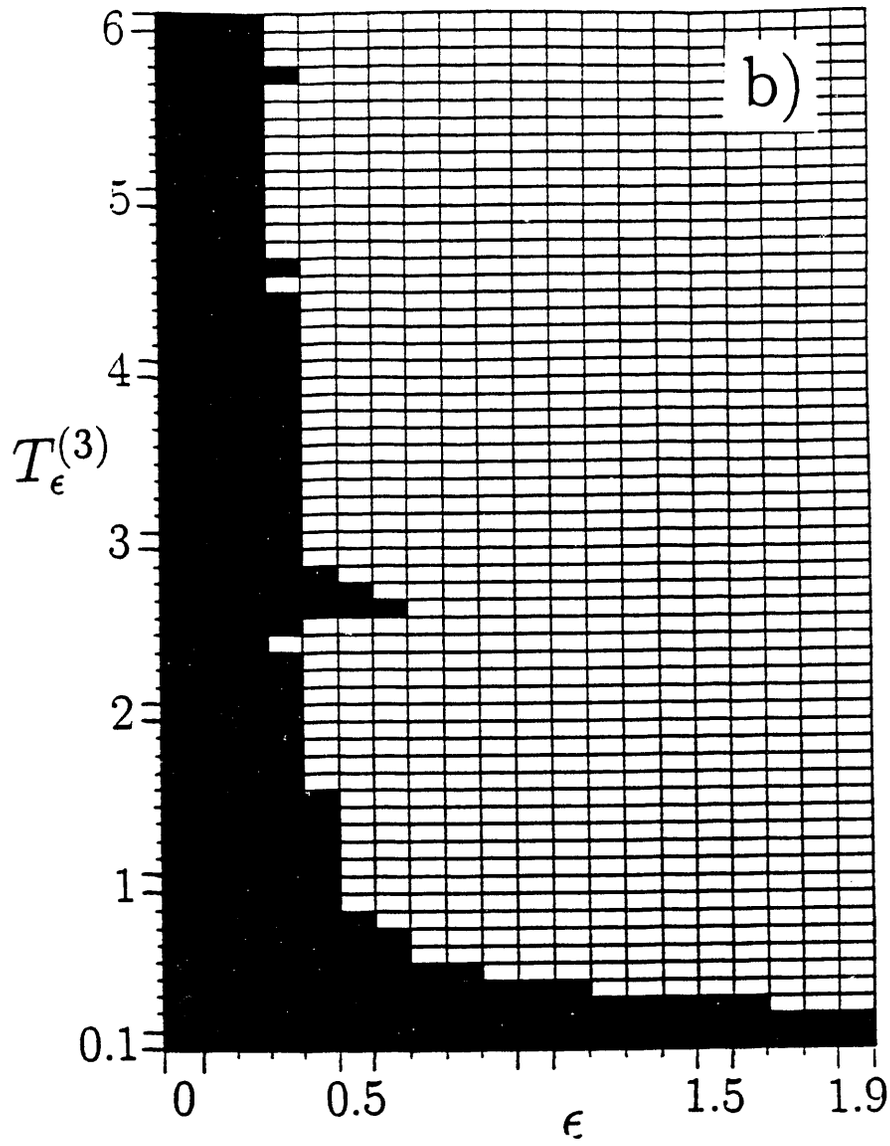
b)
6
5
4
3
2
1
0.1
$T_\epsilon^{(3)}$
0
0.5
1.5
1.9
ϵ

Fig 5c

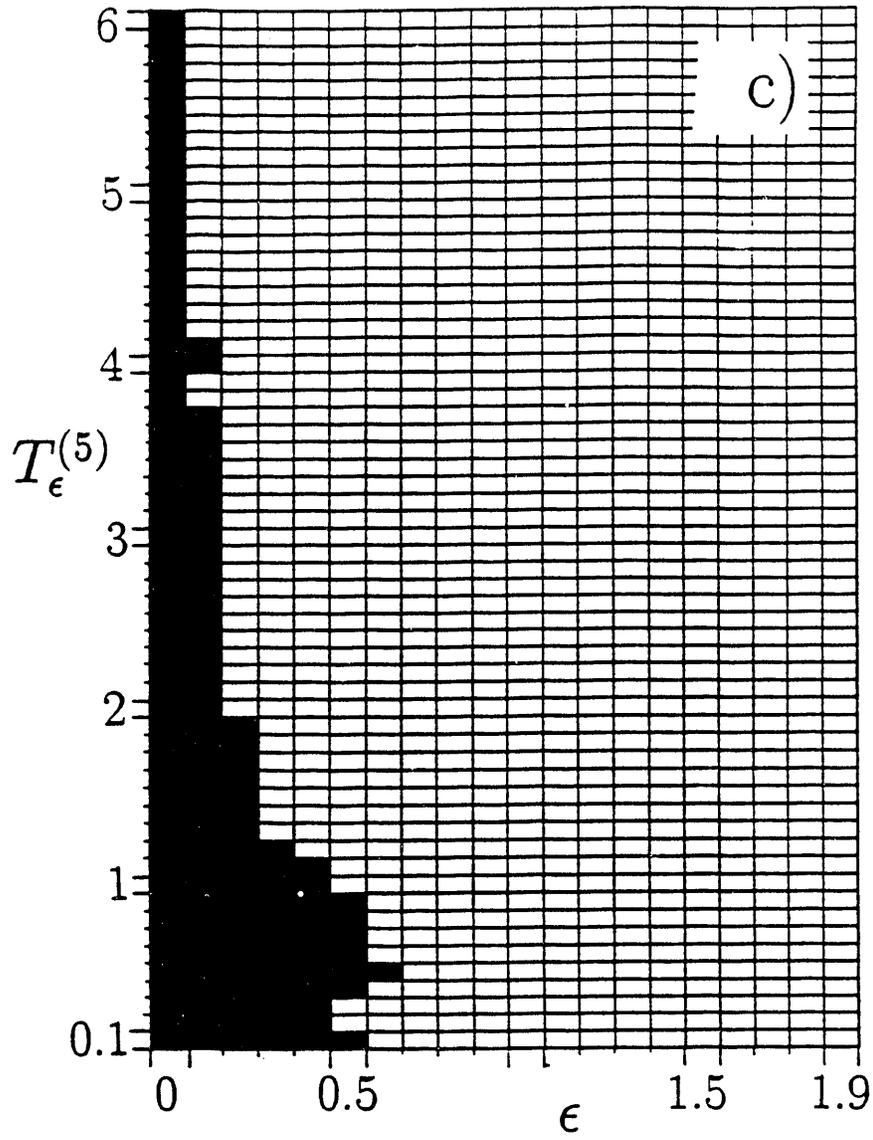

Fig. 6

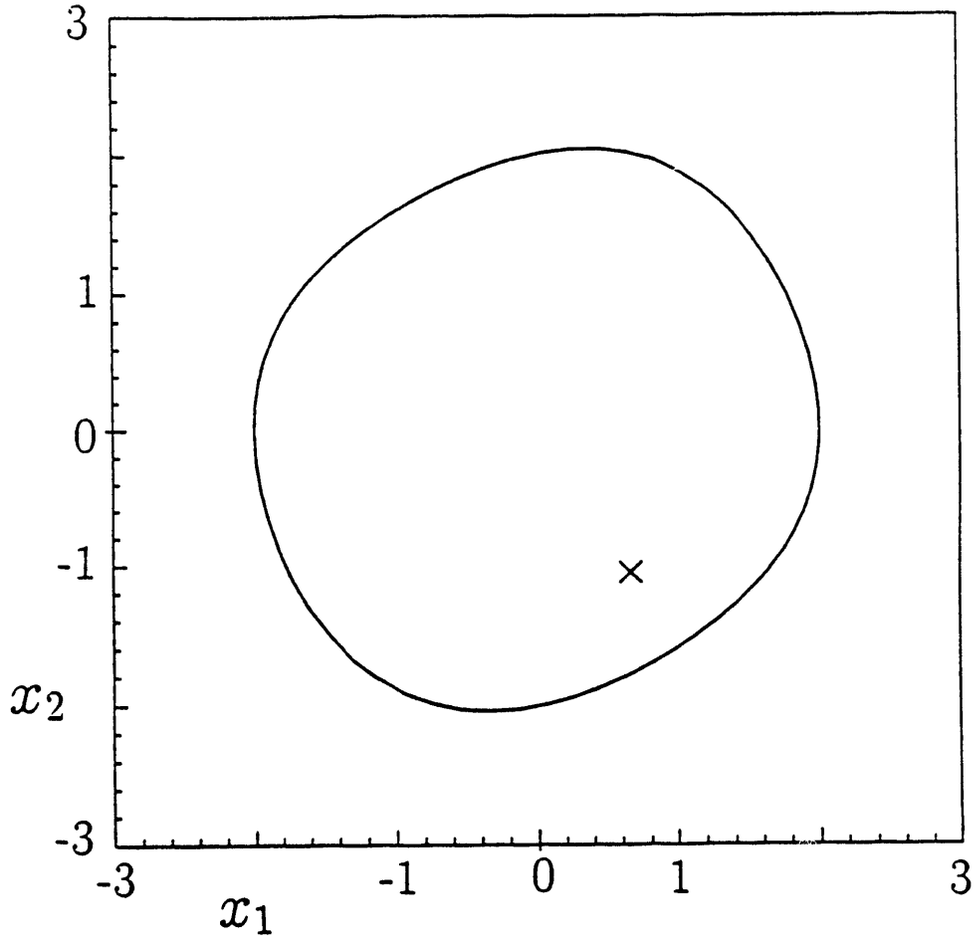

Fig 7a

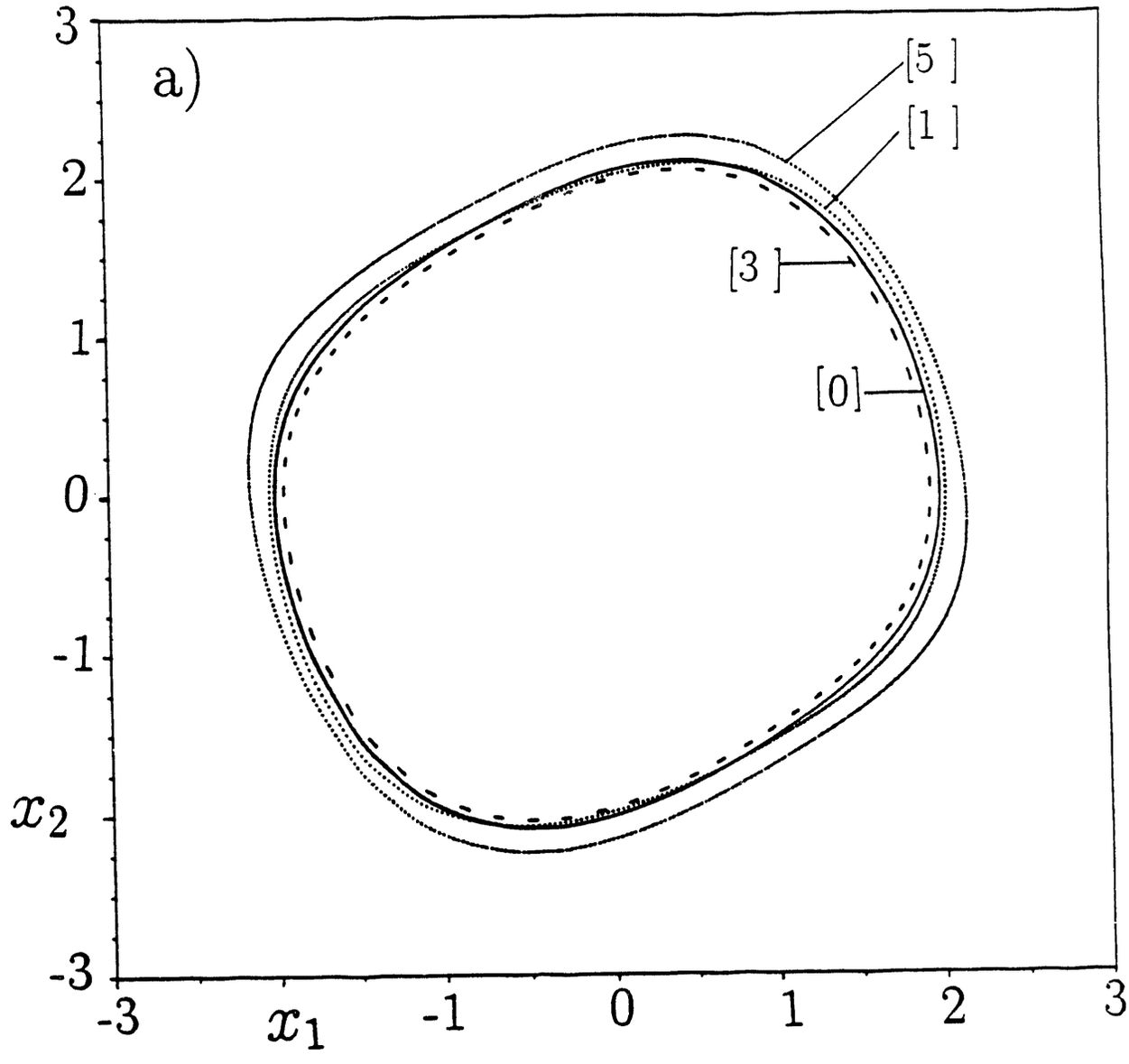

Fig 76

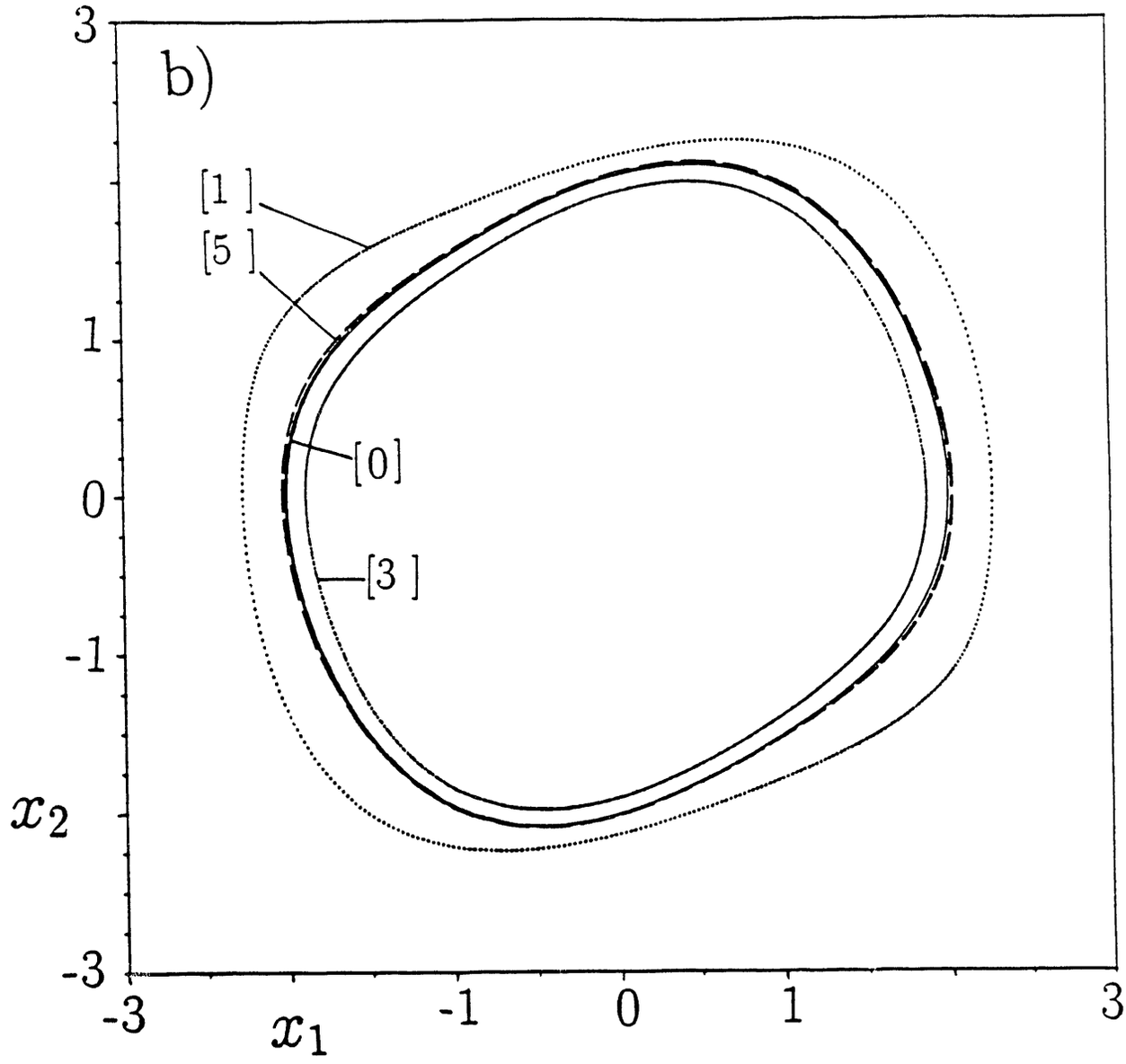

Fig 7c

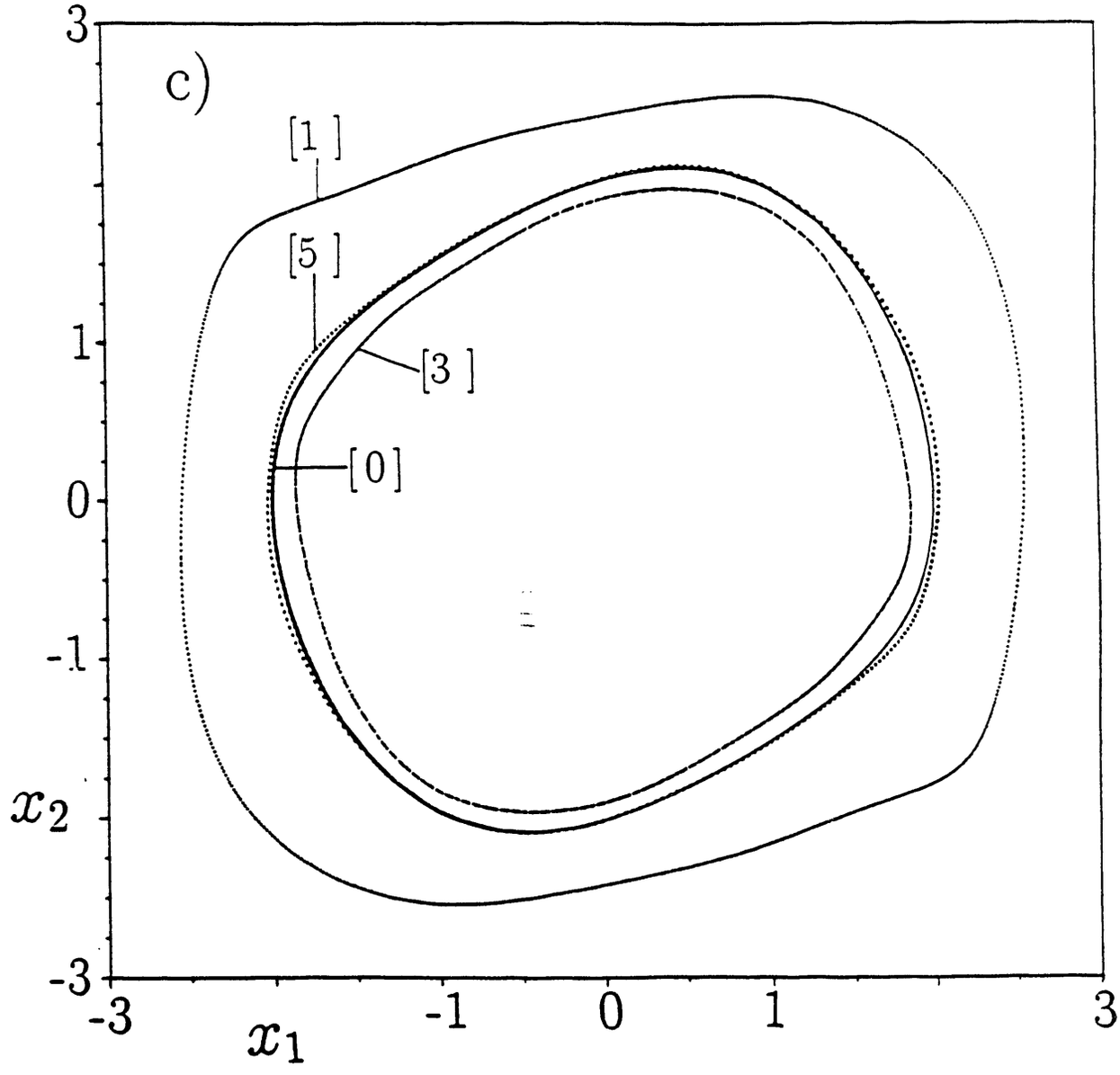

Fig. 8

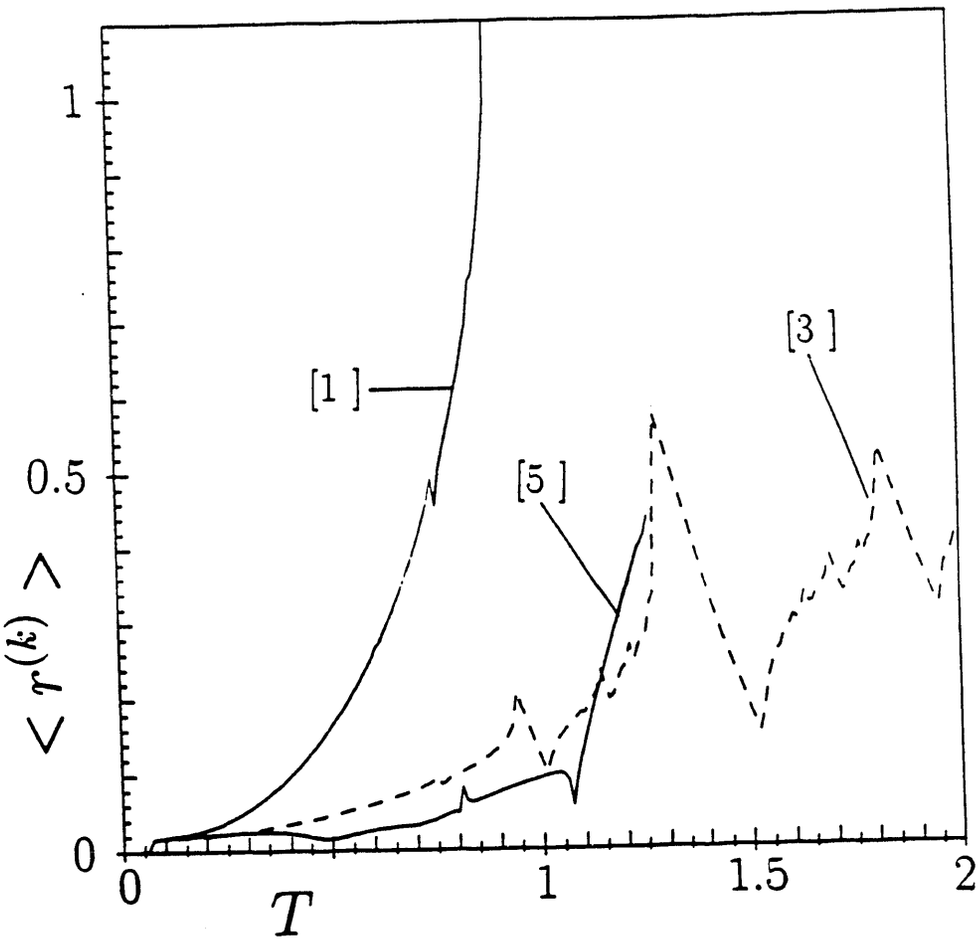

Fig 9a

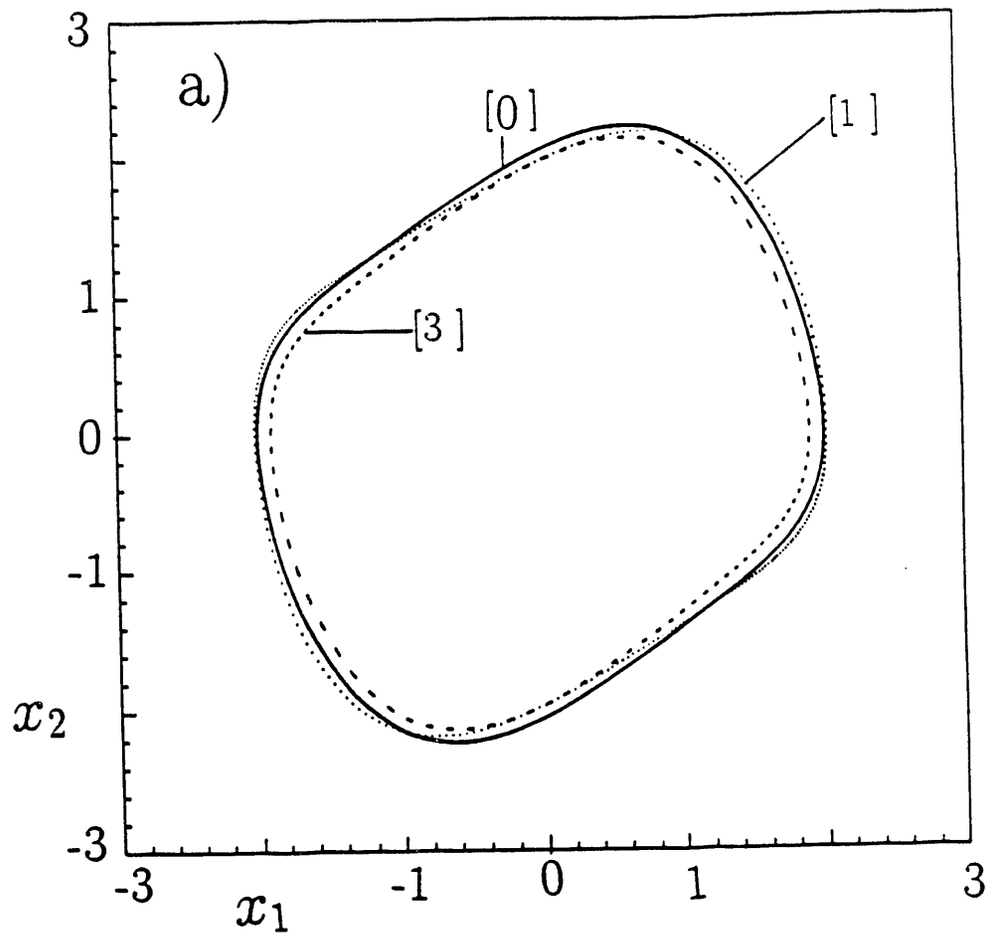

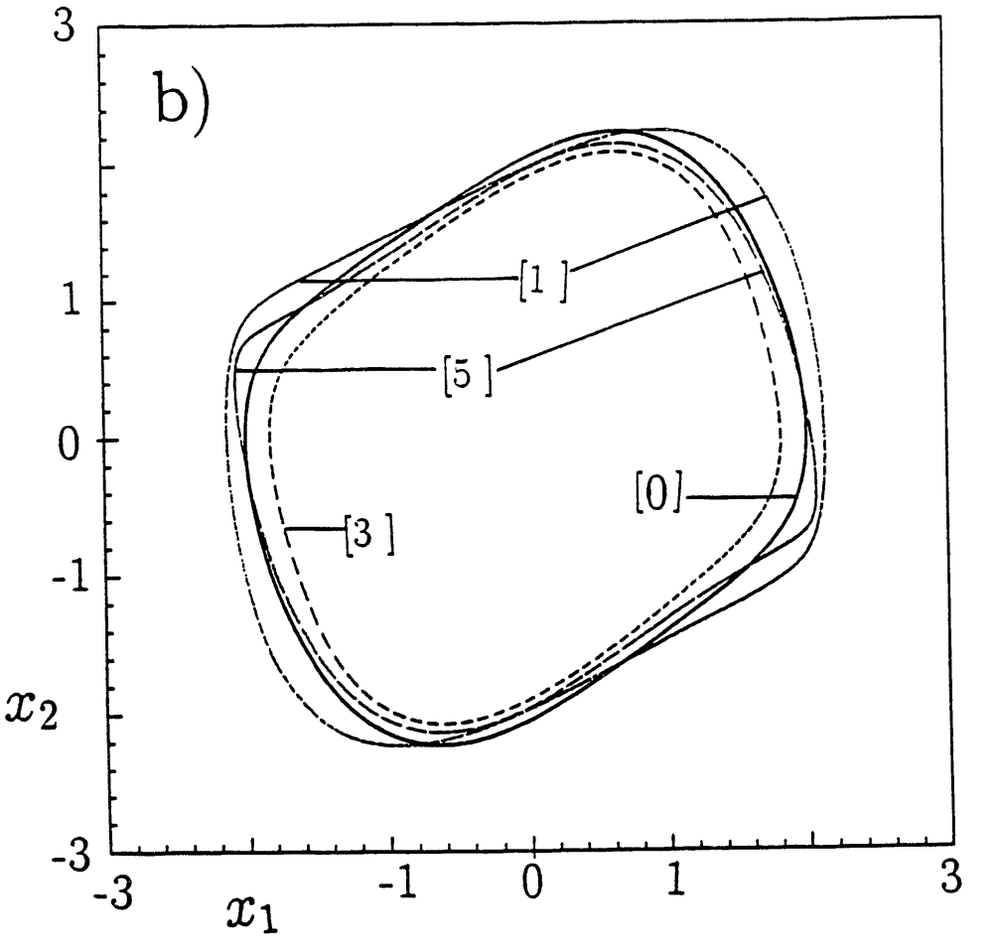
b)
[1]
[5]
[0]
[3]
3
1
0
-1
-3
-3
-1
0
1
3
x_2
x_1

Fig. 3c

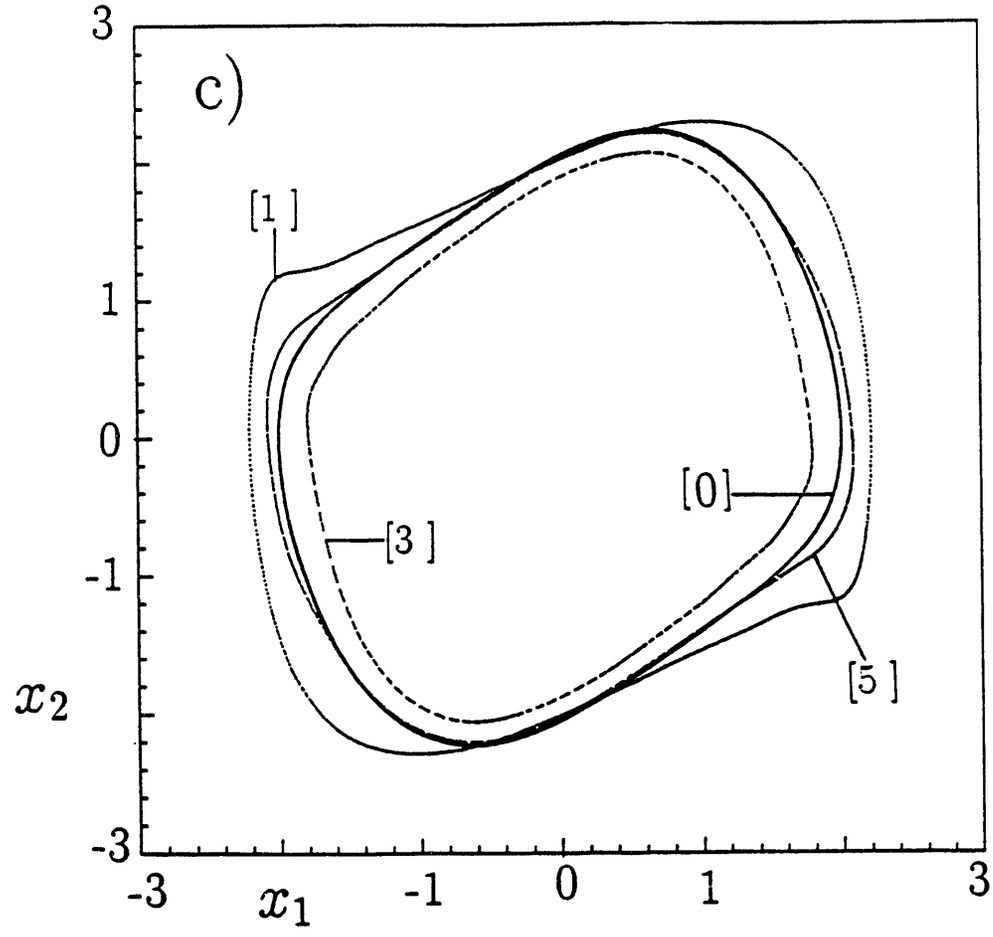

Fig. 10

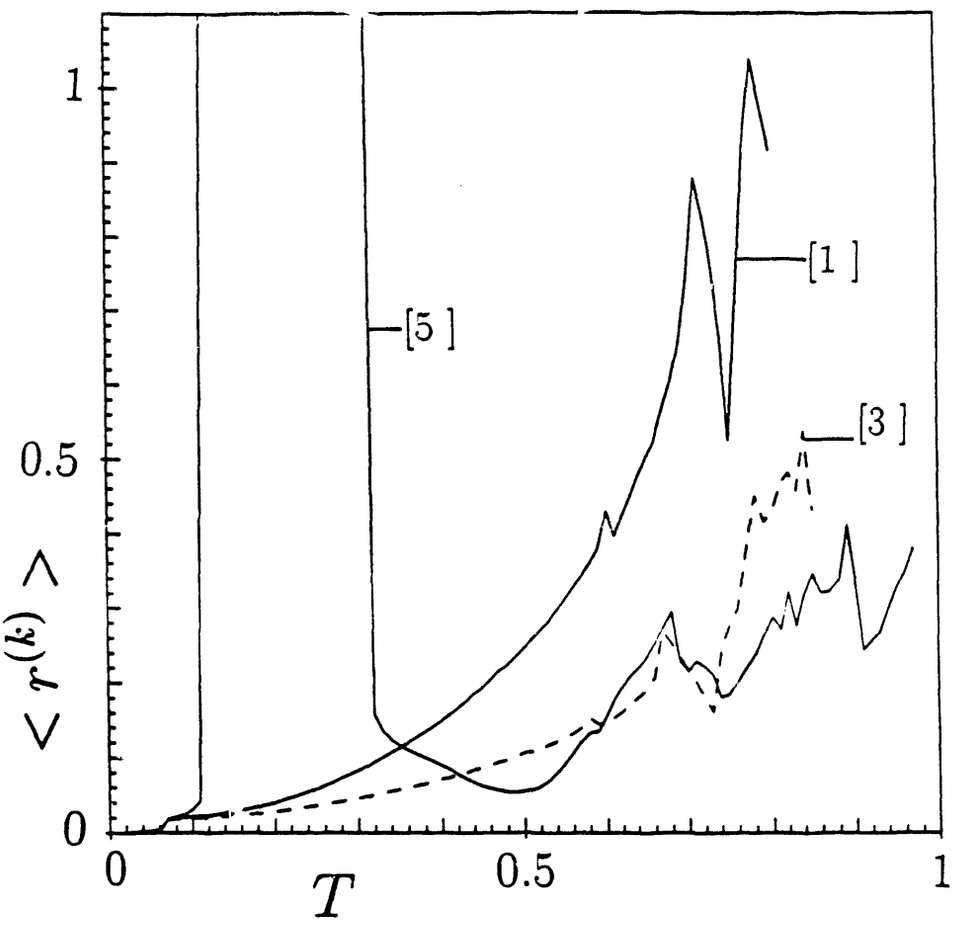

fig. 11

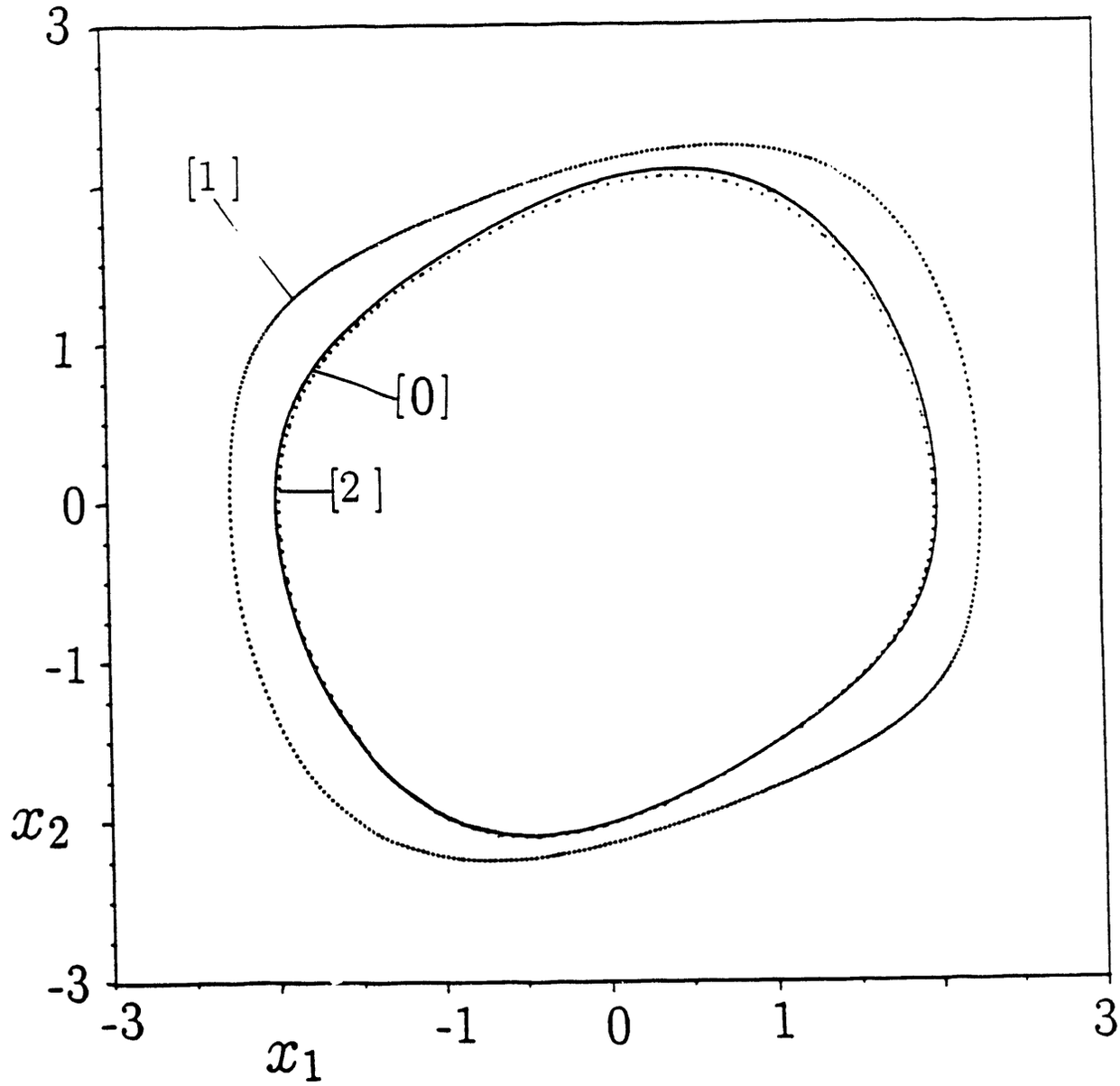

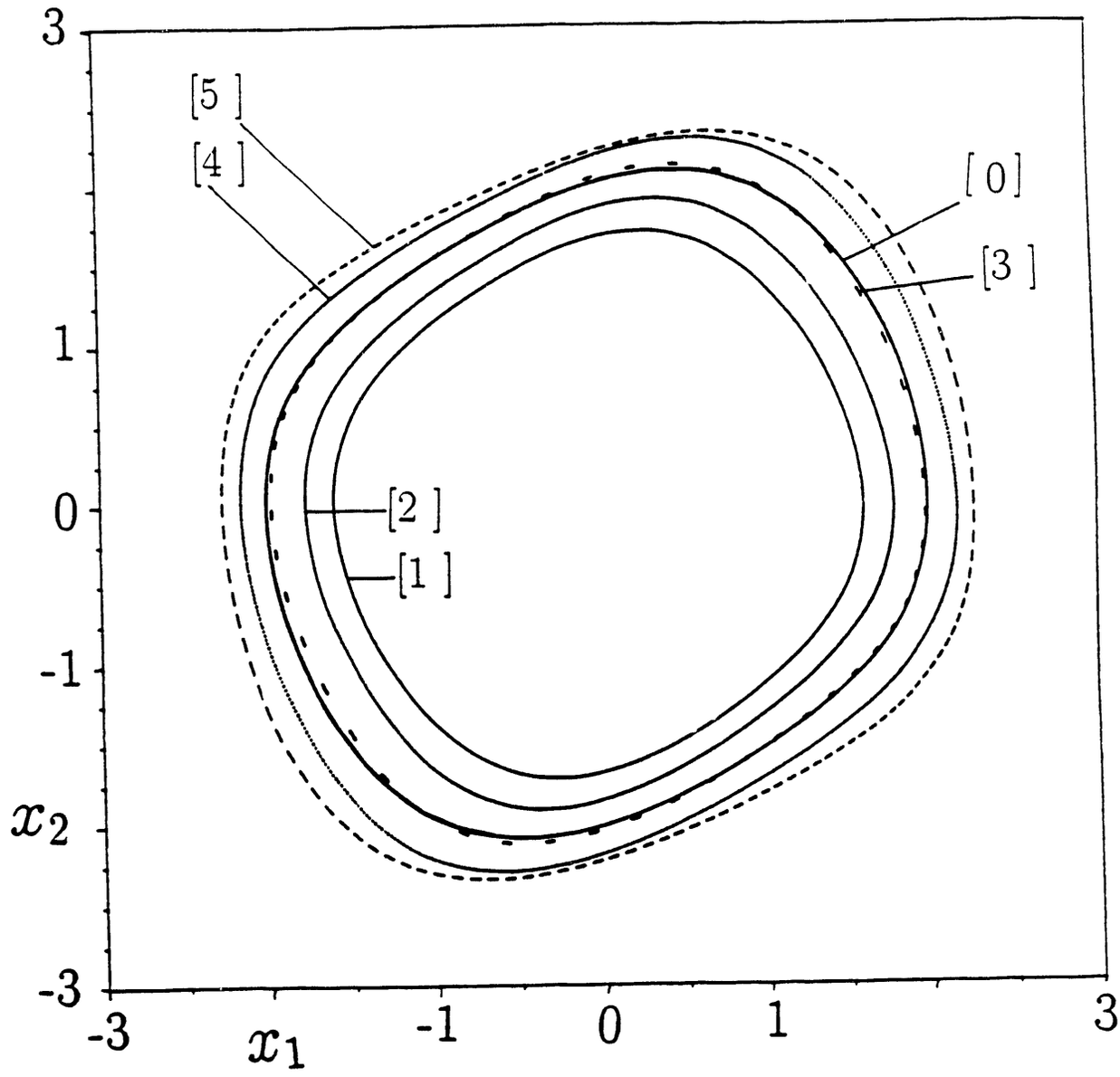
3
1
0
-1
-3
-3
-1
0
1
3
x_1
x_2
[5]
[4]
[0]
[3]
[2]
[1]

Fig 13

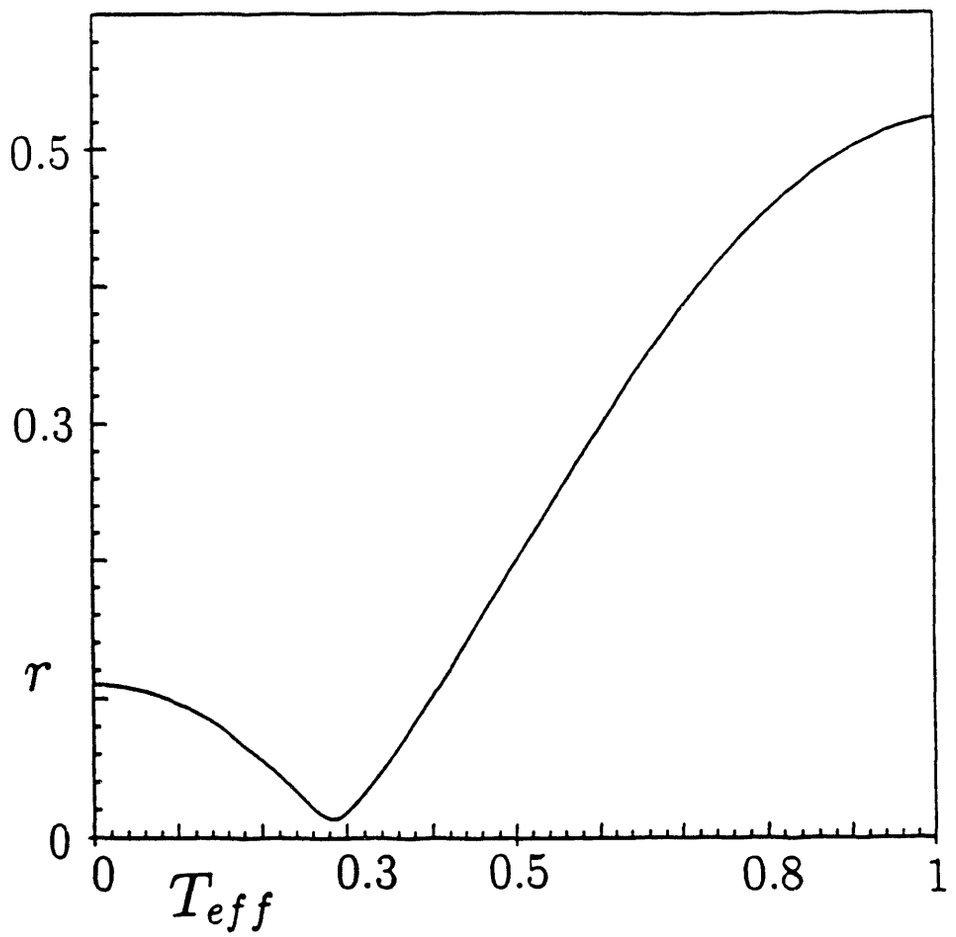

Fig 1

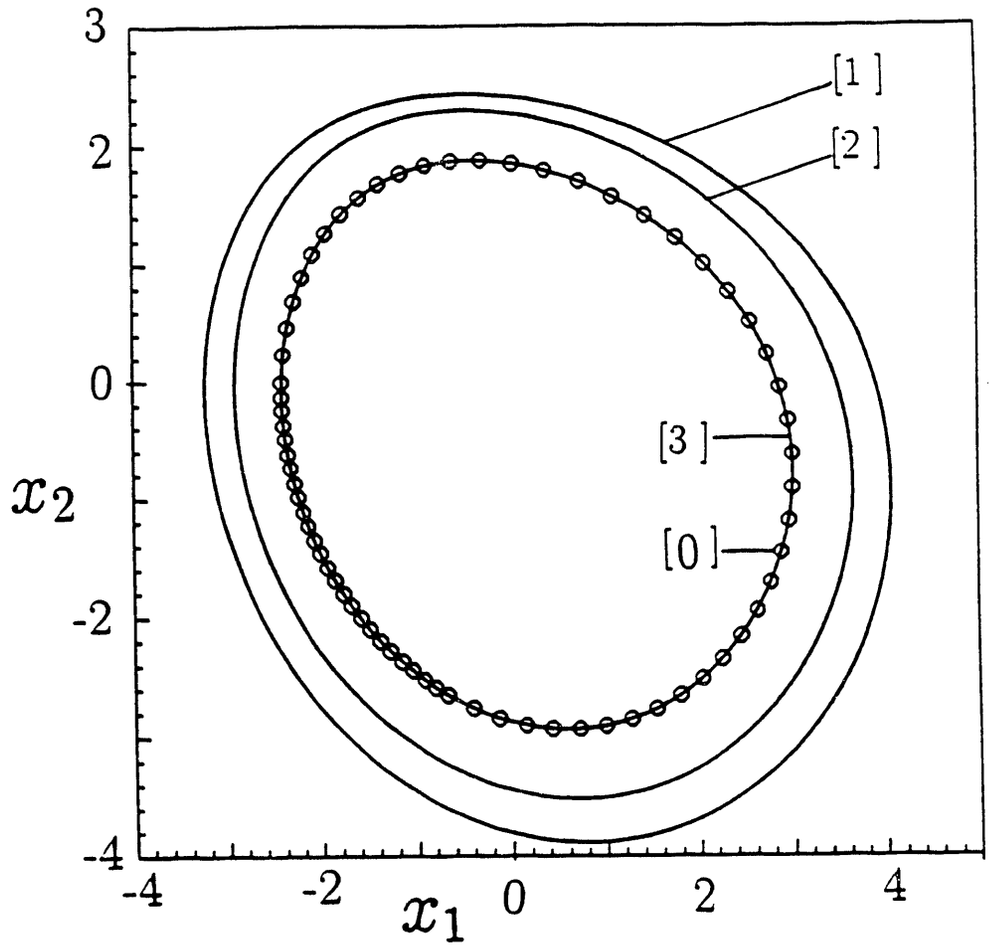

Fig 15a

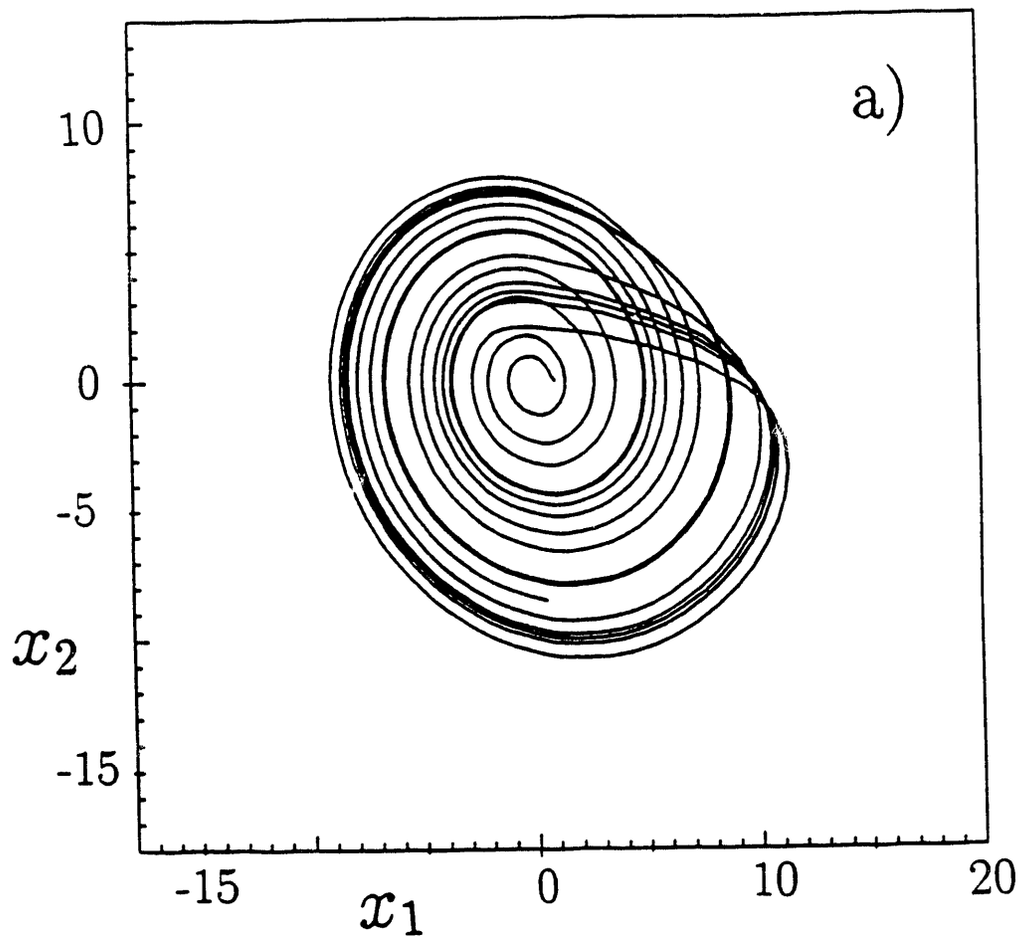

Fig. 15b

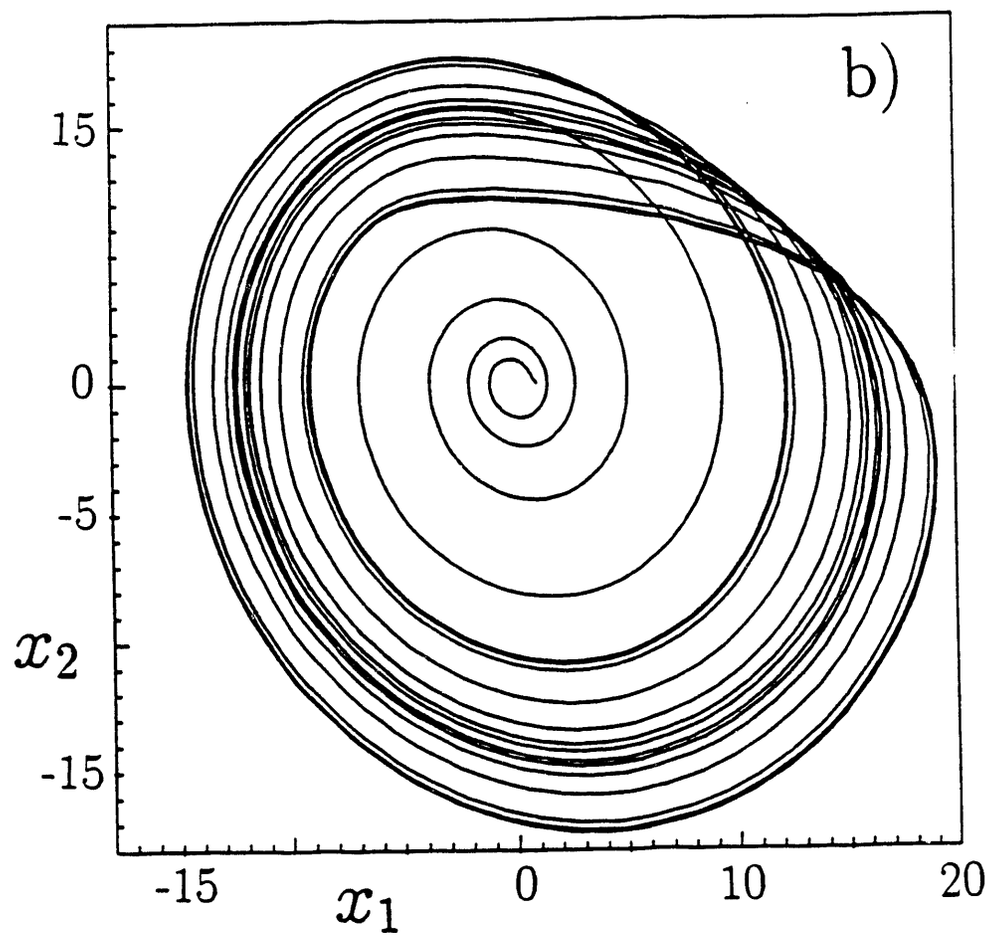

Fig. 5c

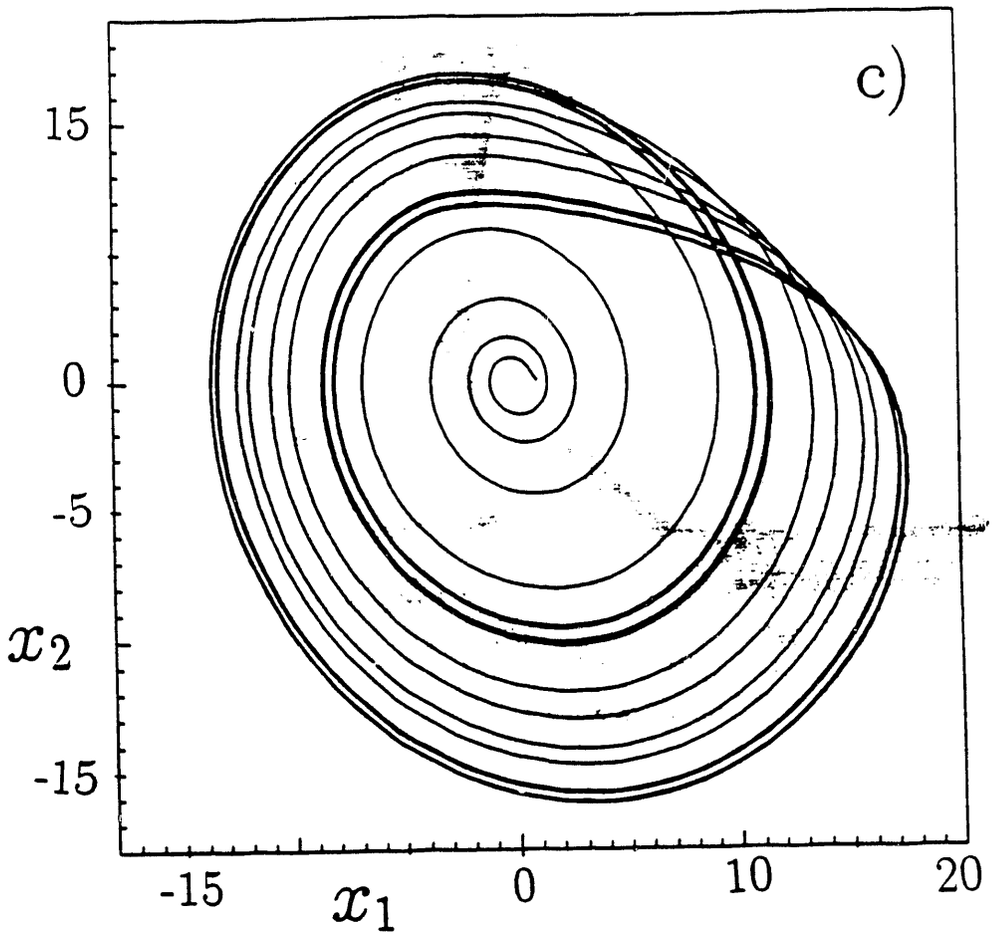

Fig. 15d

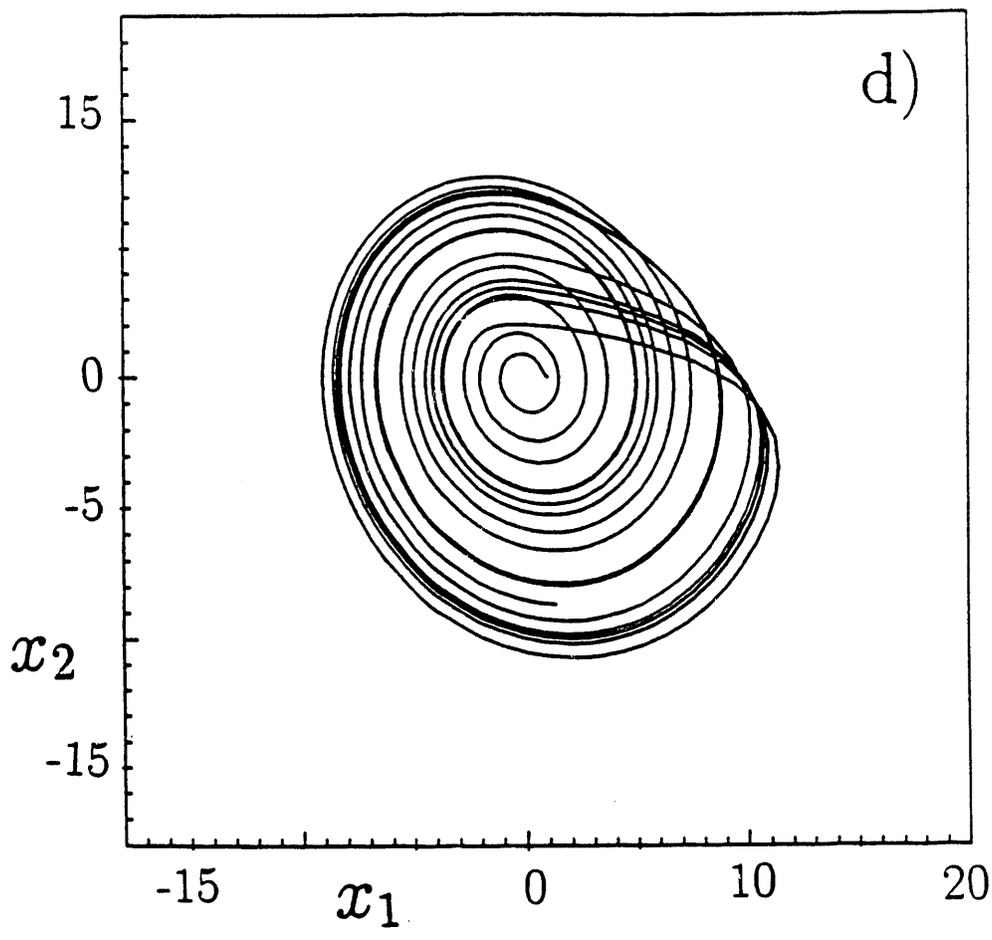

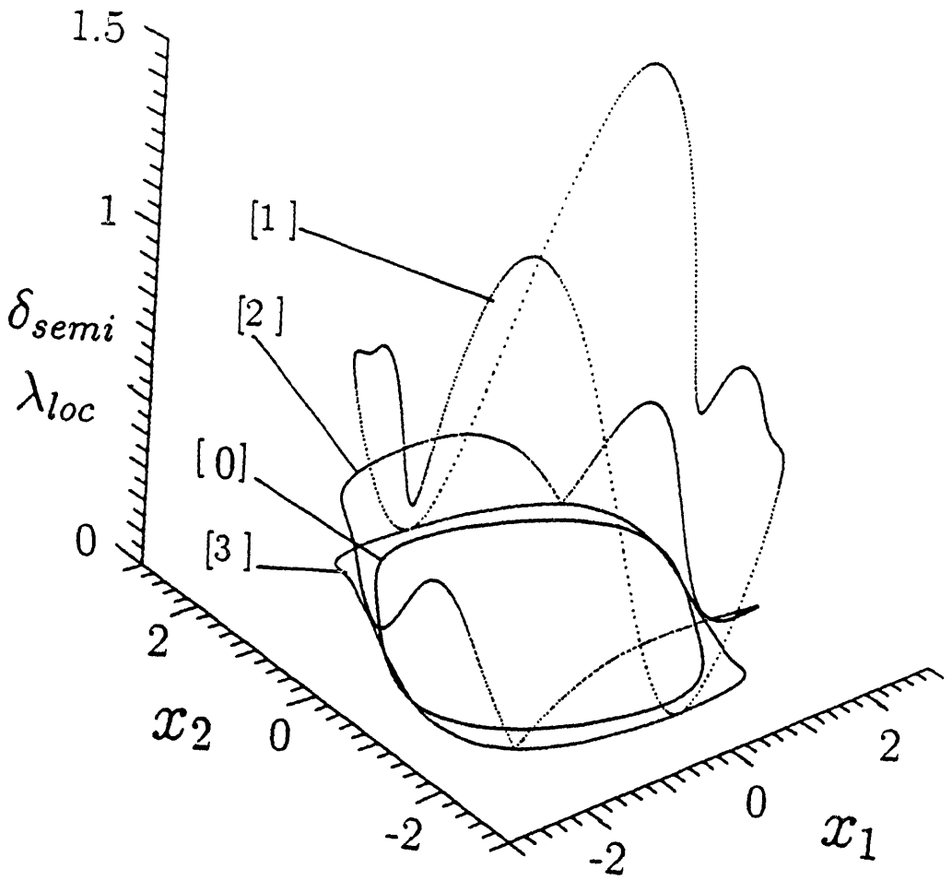
1.5
1
δ_{semi}
λ_{loc}
0
[1]
[2]
[0]
[3]
2
x_2
0
-2
-2
0
2
x_1

Fig 17

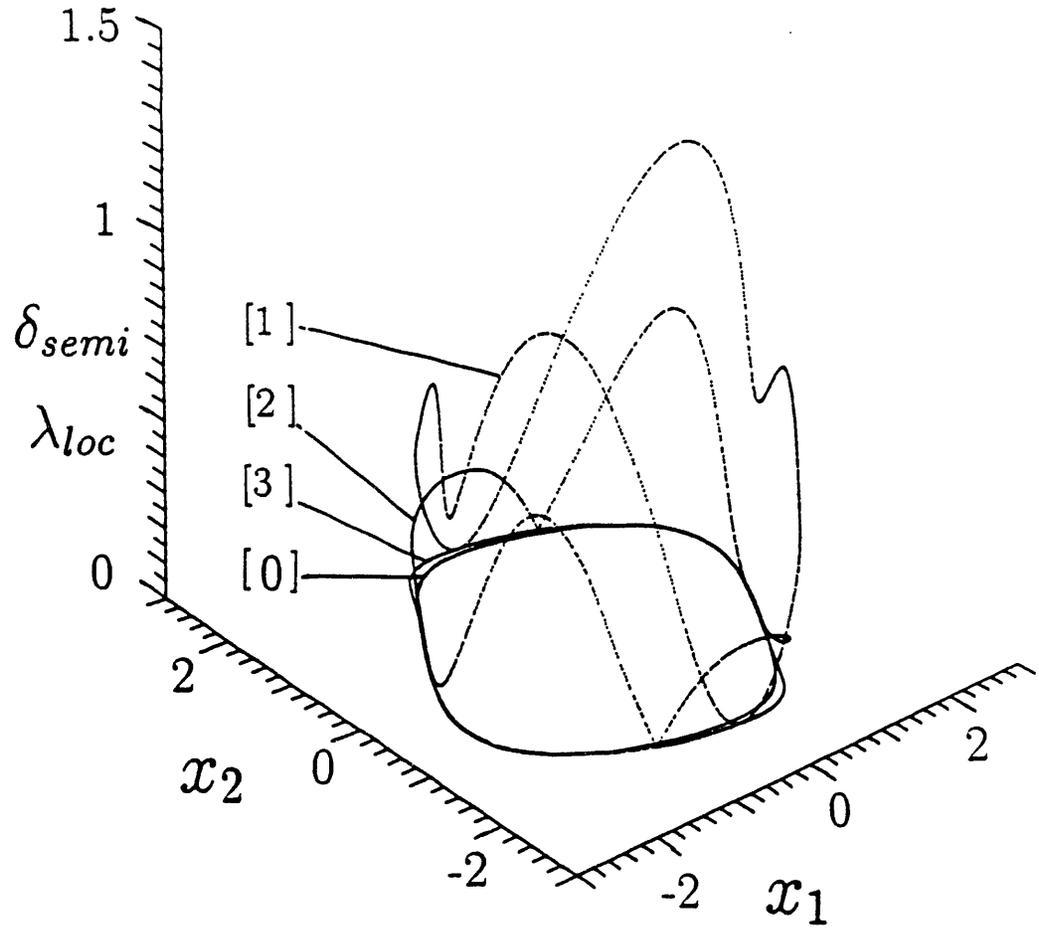

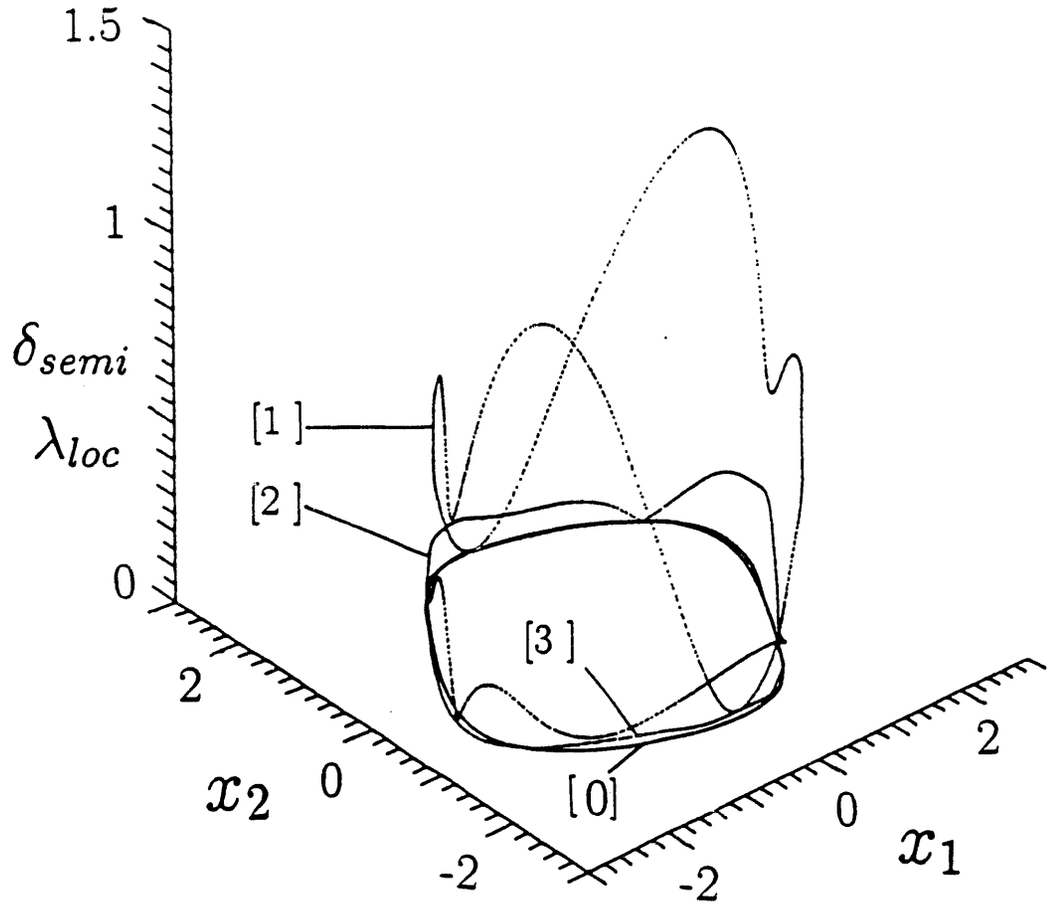
1.5
1
δ_{semi}
λ_{loc}
0
[1]
[2]
[3]
[0]
2
0
-2
x_2
2
0
-2
x_1

Fig. 19a

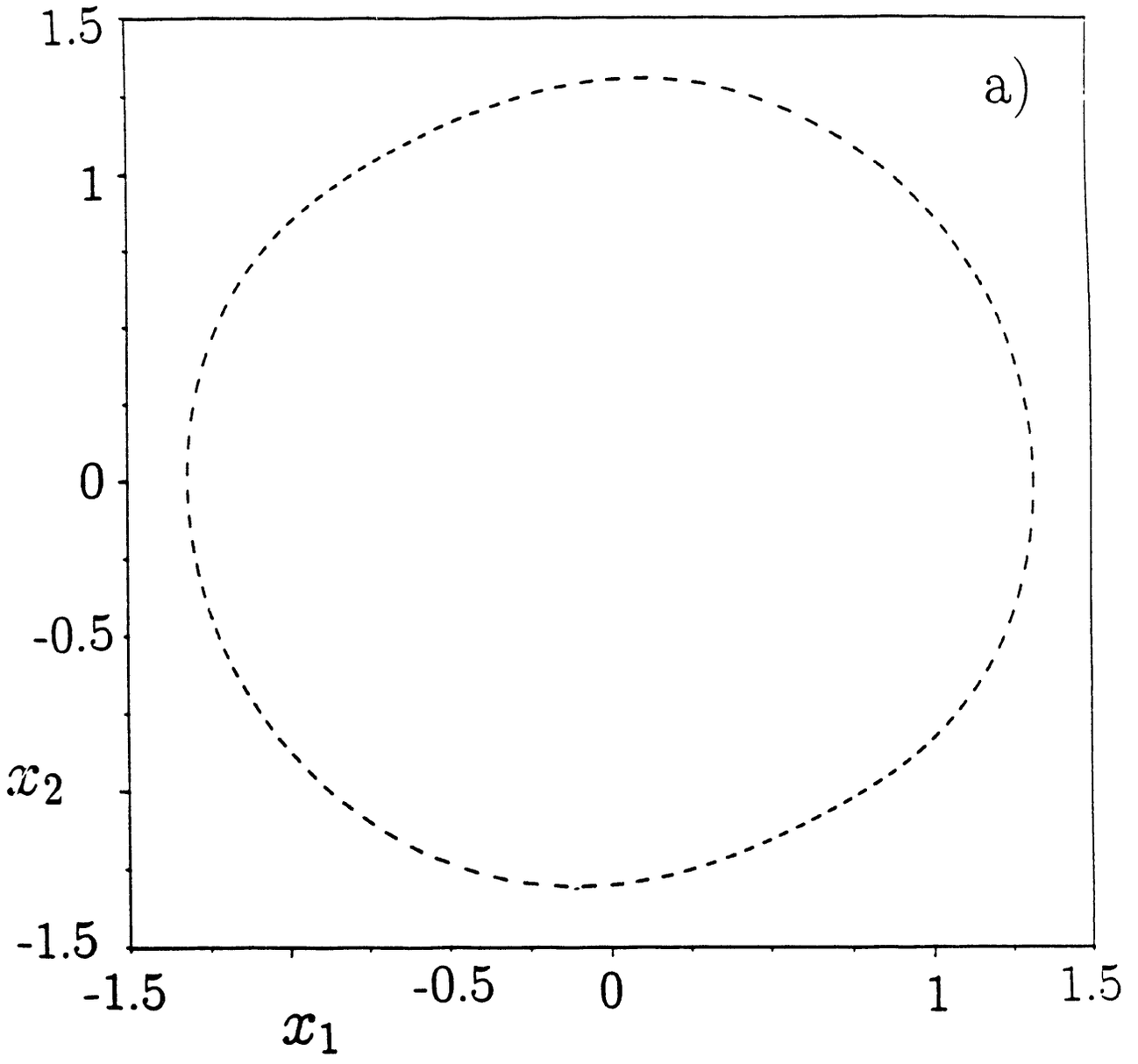

fig 5b

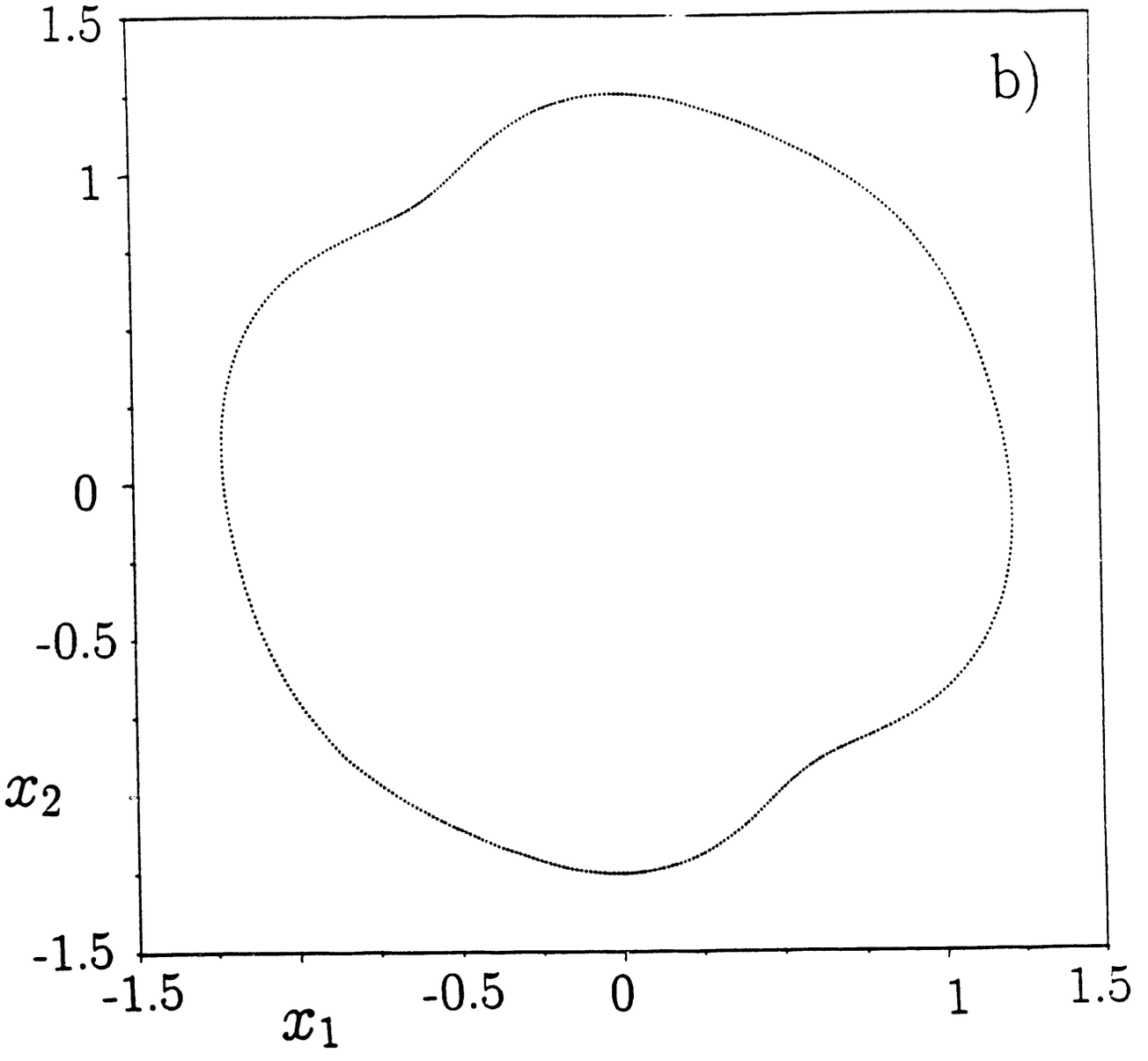

Fig 8c

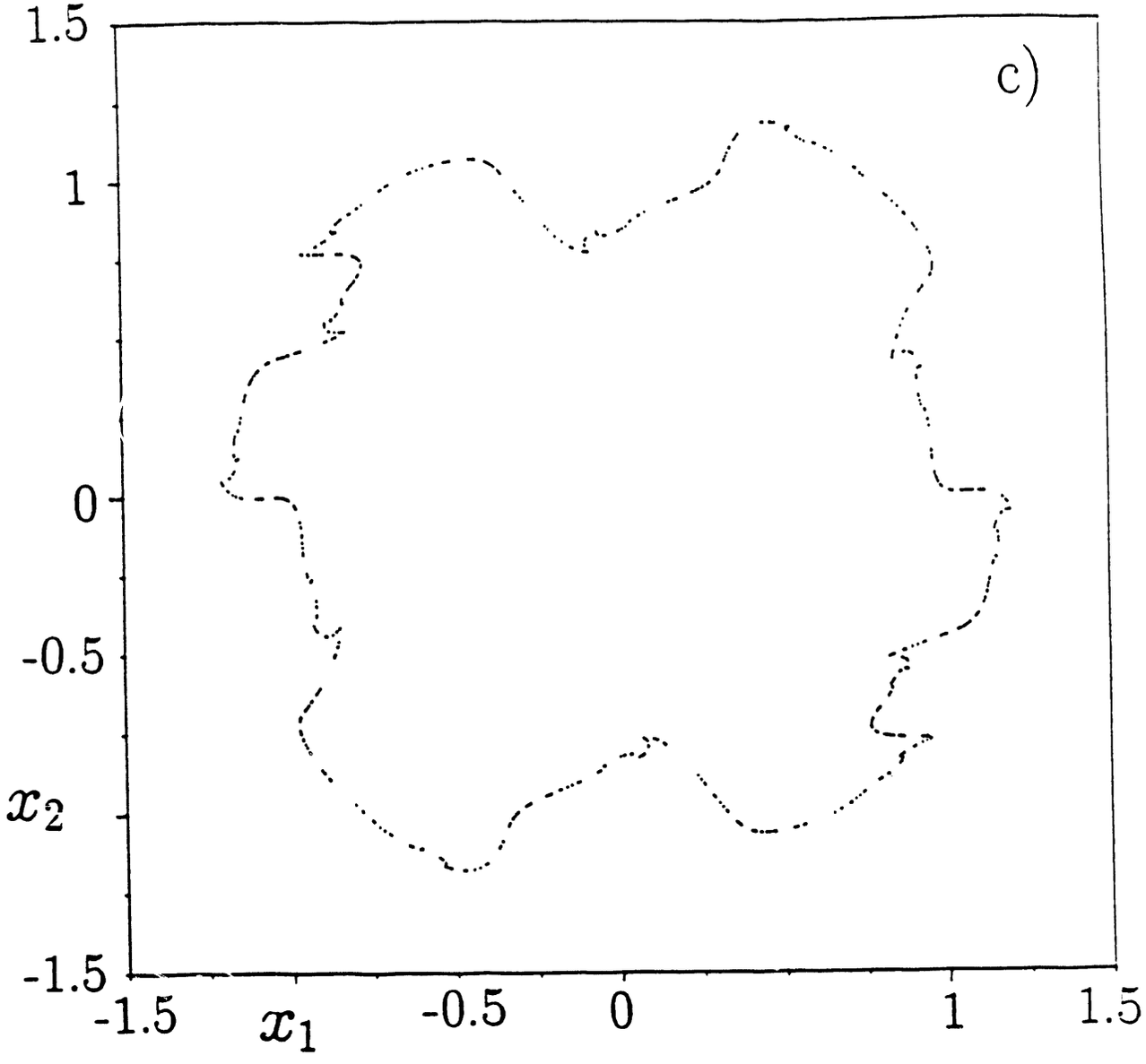

Fig 13d

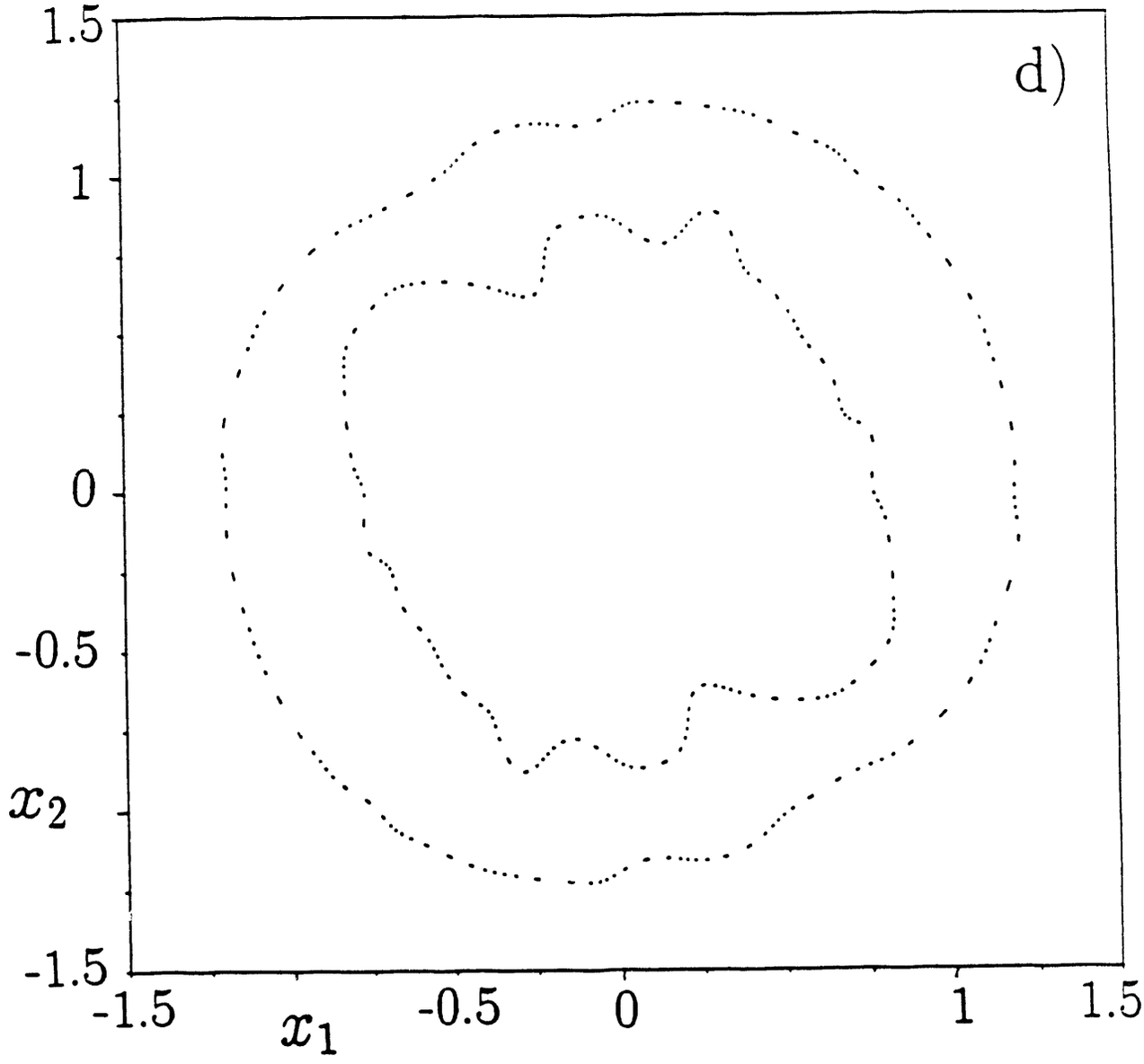

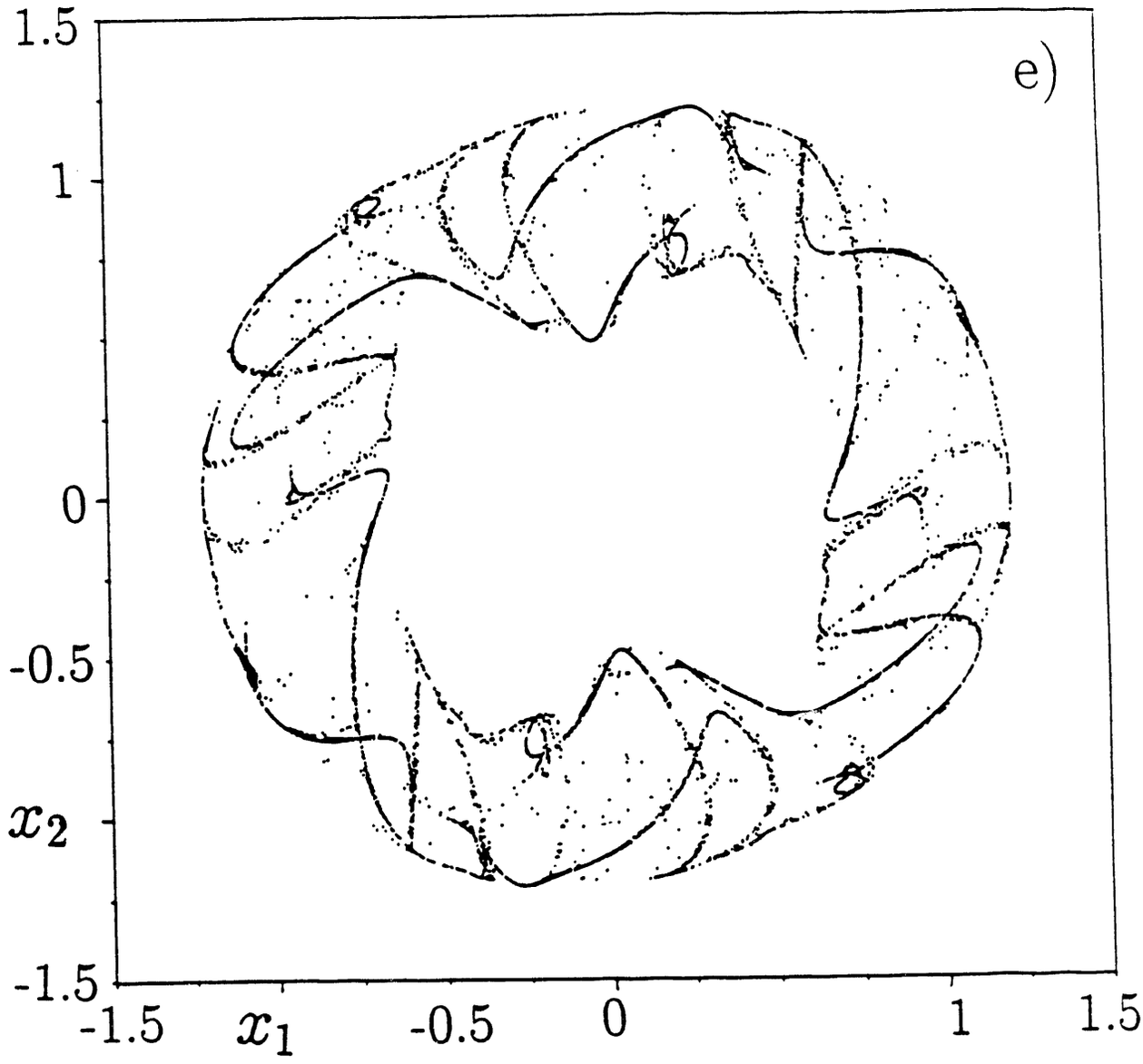
e)
1.5
1
0
-0.5
-1.5
x_2
-1.5
x_1
-0.5
0
1
1.5

Fig 19f

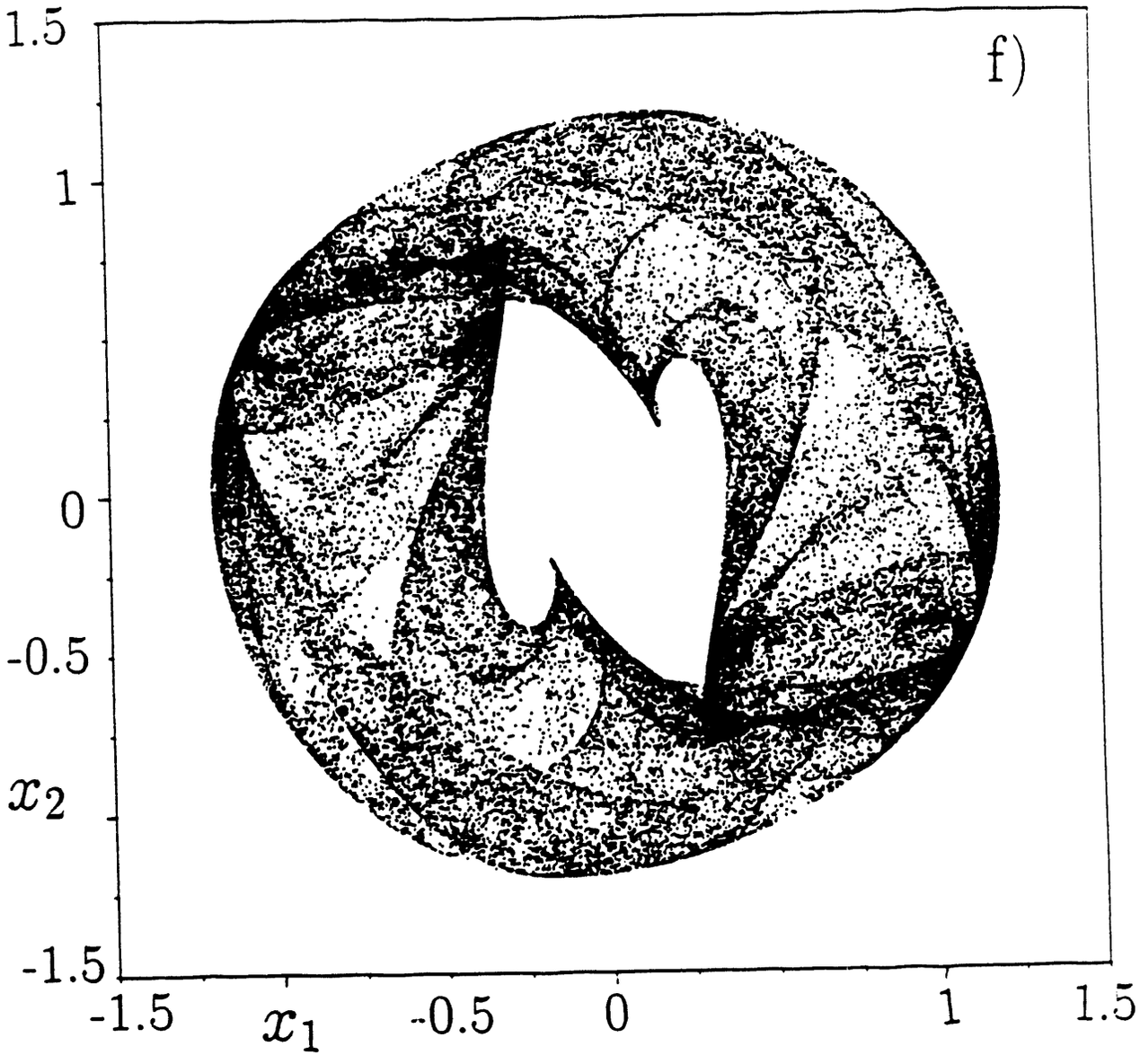

END

DATE FILMED

10/30/91